QUARTERLY REPORT

January 1, 2024 – March 31, 2024

Kentucky Tobacco
Research & Development Center

Martin-Gatton
College of Agriculture,
Food and Environment

Martin-Gatton
College of Agriculture,
Food and Environment

MEMORANDUM

DATE: April 29, 2024

TO: Kentucky Tobacco Research Board Members
Legislative Research Commission

FROM: Dr. Ling Yuan
Managing Director, KTRDC

SUBJECT: Kentucky Tobacco Research & Development Center
Quarterly Report for January 1, 2024 – March 31, 2024

Enclosed is a copy of the Kentucky Tobacco Research & Development Center's Quarterly Report for January 1, 2024 – March 31, 2024.

If you have any questions, please feel welcome to contact me at (859) 257-5798 or email lyuan3@uky.edu.

Enc.

TABLE OF CONTENTS

EXECUTIVE SUMMARY

Introduction

The legislation (KRS 248.510 - 248.580) which provides funds in support of the research programs at the Kentucky Tobacco Research and Development Center (KTRDC) requires that a quarterly research report be submitted to the Kentucky Tobacco Research Board (KTRB) and the Legislative Research Commission.

The overall reporting plan is:

January 1	-	March 31:	Selected topics
April 1	-	June 30:	Selected topics
July 1	-	September 30:	Selected topics
October 1	-	December 31:	Annual comprehensive report

As required by KRS 248.570, a financial report covering expenditures for the relevant proportion of the July 1, 2023 – June 30, 2024 fiscal year is included in this report.

The news and research publications provided in this quarterly report are a representative selection of the Center's output. For a full description of all KTRDC research and activities please refer to the KTRDC Annual Report.

Quarterly News

- The emphasis in KTRDC's research work continues to be on harm reduction. There is a great deal of collaboration between field and molecular researchers, where the molecular biologists attempt to explain field observations at the cellular level. Examples of these collaborations are:
  - Both field and molecular researchers are studying the different effects of potassium chloride vs. potassium sulfate on TSNA accumulation, trying to understand the mechanism of this phenomenon.
  - There has been a significant amount of work on tobacco terpenes, such as the CBT diols. These compounds are of interest because of their effect on tobacco flavor and aroma, and also because they play a role in repelling insects. Molecular scientists are now working on the regulation of terpene formation.
  - A large part of the KTRDC research program, both field and molecular, is devoted to nicotine, particularly lowering plant nicotine levels.

- Field and molecular scientists are collaborating to try to understand why the low-alkaloid tobacco lines have such poor leaf quality. It seems that the buildup of nicotine precursors may play a role.
- Field researchers have discovered a novel low nicotine gene, which when combined with the *nic1nic2* genes in the LA lines, lowers nicotine content considerably. Molecular scientists are collaborating in an attempt to determine the mode of action of this gene.

- Work at the farm focused mainly on stripping, grading, sampling and sample preparation, chemical analysis, and seedling production.
  - Stripping was completed in mid-March and the last quality evaluation was done a week later. Stemming, drying, and grinding the samples for leaf chemistry analysis is ongoing. There has not been an adequately long window between processing the tobacco and having a long enough dry spell to strip the *Artemisia*.
    - The yield of the LA (low-alkaloid) lines was acceptable, but the quality was characteristically poor with a grade index of 30–50, mainly due to a significant proportion of green grades which were very noticeable even at stripping. The grade indices of the checks were just over 70.
    - The yield of the dark burley lines was generally good, but the quality was very variable, depending on the weather during the first few days after harvest, regardless of when these lines were topped.
  - Seeding of the tobacco for the 2024 crop was done on March 19 and 29.
  - The *Artemisia* will be seeded in April.

- The March board meeting was held in-person in the KTRDC conference room and by Zoom on March 18th 2024.
  - Ms. Kimberly Foley of Foley Seeds and Services gave a presentation entitled "A Seed Company's take on 21st Century Tobacco Production in the United States".
    - She outlined a bold vision for the future of burley tobacco production in Kentucky, predicting that Kentucky will produce 100 million pounds of burley annually by the end of the third decade of the 21st century, reflecting a commitment to growth and sustainability.
    - To capitalize on this market, Ms. Foley stressed the importance of understanding customer needs and forming strategic partnerships that are aligned with the company's vision.

    - Ms. Foley also highlighted several primary risks facing US burley production, including reliance on domestic markets, competition from lower-cost sources, production costs, and regulatory challenges.
  - Dr. Yuan gave an update on the budget.
    - He noted that there has been a reduction in tax income from last year and it has been trending downward for at least the past five years.
    - Dr. Yuan stated there has been a gradual downward trend in funding over the past five years. There were three FDA grants to develop tobacco reference products over the years that helped support personnel, but the last grant is ending. KTRDC will need to use reserve funds, but reserve funds will not sustain the Center in the long term.
    - Dr. Yuan then gave a KTRDC update and talked about the Cannabis Center Collaboration. KTRDC has a small, secure growth chamber which will be used to produce cannabis for the Cannabis Center. The chamber is currently being tested with hemp plants.
  - The chairman outlined the board governance items, clarifying issues such as voting and member structure.
- KTRDC scientists are closely involved with CORESTA.
  - KTRDC scientists lead three CORESTA subgroups and participate in many more.
  - One KTRDC scientist has been chosen to participate in the CORESTA Tobacco Harm Reduction (THR) Committee, representing the supply chain (key focus area 3 below). The committee has identified five major focus areas for harm reduction, most of them relating to the human aspects of tobacco use.
    1. Risk reduction to harm reduction
    2. Real world evidence on potentially reduced risk products (PRRPs) in the context of global regulations
    3. Supply chain considerations in THR
    4. Developing and applying new methods/techniques/models to assess potentially reduced risk product across all science areas
    5. Nicotine science – health effects and misperceptions
    - The committee will hold its first meeting in May in Toronto.
- The Tobacco Workers Conference was held in Knoxville, Tennessee in January. Several KTRDC scientists attended and presented papers.

- The calls for papers for the two major conferences have gone out.
  - The CORESTA call for papers was sent out in March, for the Congress to be held October 13th – 17th in Edinburgh, Scotland. Abstracts, due in mid-May, are being prepared and several KTRDC scientists will attend. The congress theme is "Advancing Tobacco Harm Reduction through Scientific Collaboration".
  - The call for papers for the 77th TSRC conference went out in March. The conference will be held September 8th – 11th in Atlanta, Georgia. The theme is "Tobacco Harm Reduction: What Have We Learned and How Do We Move Forward?" Abstracts, due in mid-May, are being prepared and several KTRDC scientists will attend.
- The CTRP proficiency testing (PT) program currently covers the certified 1R6F reference cigarette and the certified reference smokeless tobacco products.
  - The current PT rounds are:
    - SMK-2023D – The parameters for this round of testing include Total Nicotine, Free Nicotine, Nicotine-derived Nitrosamine Ketone (NNK, (4-(methylnitrosamino)-1-(3-pyridyl)-1-butanone)), N'-nitrosonornicotine (NNN), N'-nitrosoanatabine (NAT), N-nitrosoanabasine (NAB), Acetaldehyde, Crotonaldehyde, Formaldehyde, Benzo[a]pyrene (BaP), Cadmium, Arsenic, pH and Moisture, using two certified reference smokeless tobacco products: 1S5 (Snus) and 3S1 (Loose Leaf Chewing Tobacco). This round of testing opened in August 2023 and the data portal for participants to upload data closed March 2024. The interim report was released for participant review in March 2024 and the final report will be released in April 2024.
    - CIG-2024A – The parameters for this round of testing include smoking parameters o-toluidine, 2,6-dimethylanilin, o-anisidine, 1-aminonaphthalene, 2-aminonaphthalene, 3-aminobiphenyl, 4-aminobiphenyl, Total Particulate Matter (TPM), Puff Count, Benzo[α]pyrene (BaP), BaP-Total Particulate Matter (BaP-TPM) and BaP-Puff Count Parameters using the 1R6F reference cigarette as proficiency test material smoking in both the non-intense and intense smoking regimes. This round of testing opened in January 2024 and the data portal for participants to upload data closed March 2024. The interim report was released for participant review in March 2024 and the final report will be released April 2024.

- CIG-202BA – The parameters for this round of testing include smoking parameters Ammonia, Acrylonitrile, Isoprene, Benzene, Toluene, 1,3 Butadiene, Total Particulate Matter, and Puff Count using the 1R6F reference cigarette as proficiency test material smoked in both the non-intense smoking regime and the intense smoking regime. This round of testing opened in March 2024 and the data portal for participants to upload data will close in June 2024.

- Two of the three Food & Drug Administration (FDA) grants awarded to the University of Kentucky, Center for Tobacco Reference Products (CTRP), to produce and distribute reference tobacco products are now complete: the Cigarette Tobacco Reference Products (RFA-FD-14-001) and the Smokeless Tobacco Reference Products (RFA-FD-15-026). There is progress to report this quarter on the Cigar Tobacco Reference Products (RFA-FD-20-002) grant.
  - Cigar Tobacco Reference Products Program (RFA-FD-20-002): The COVID pandemic significantly impacted this project and led to delays in the manufacturing, characterization, and distribution schedule set forth in the grant proposal timeline.
    - Three ISO 17025 accredited labs (Labstat, Global and Enthalpy) have completed the characterization process for the large cigar (1RLC) manufactured by ITG Brands (Imperial Tobacco Group). These laboratories have completed the physical measurements and chemical analysis based on the requirements and list of Harmful and Potentially Harmful Constituents (HPHCs) set forth in the grant. The CTRP has finalized the Certificate of Analysis (CoA) and the FDA has reviewed and approved the CoA for distribution to the research community. The CTRP also prepared and submitted to the FDA a Homogeneity Analysis Report for the 1RLC, including six-months of long-term stability analysis data. The 1RLC is listed on the CTRP website and is available for purchase by tobacco research scientists.
    - Two of the three ISO 17025 accredited labs (Labstat and Enthalpy) have completed the characterization process for the cigarillo/small cigar (1RSC) manufactured by Swedish Match. Labstat and Enthalpy followed the CTRP protocol for the physical measurements and chemical analysis based on the requirements and list of HPHCs set forth in the grant.

- Two of the three ISO 17025 accredited labs (Labstat and Enthalpy) have completed the characterization process for the filtered cigar (1RFC) manufactured by Scandinavian Tobacco Group (STG).
- The CTRP was notified by Global that the company was going out of business and would not be able to perform the characterization analysis on the 1RSC or the 1RFC. The CTRP began an extensive process of exploring options to contract with an ISO 17025 accredited laboratory to replace Global as the third analytical laboratory. Additionally, the CTRP was notified on November 27, 2023, that Enthalpy was being acquired by McKinney Specialty Labs (MSL), with the transaction scheduled to close prior to year-end. MSL acquired the analytical equipment, retained the personnel of Enthalpy, and the ISO accreditations were transferred to MSL.
- After a lengthy due diligence process, including discussions with commercial laboratories, manufacturers, and other institutions, and in consultation with the FDA, it was decided that the best path forward was to contract with Labstat and MSL to conduct additional characterization for the 1RSC (cigarillo) and the 1RFC (filtered cigar), following the CTRP protocol for the physical measurements and chemical analysis of constituents based on the requirements and list of HPHCs set forth in the Collaborative Agreement. Based on this option, the CTRP will be obtaining four data sets by using both labs (Labstat and Enthalpy/MSL) to test the 1RSC and 1RFC, which will produce sufficient data to establish a true data range for the analytes, thereby creating a better understanding of the variability of these cigar analytes and physical parameters.
- Due to budget constraints and the additional characterization agreed on, the CTRP requested additional funding for the cigar project in the amount of $484,609 to successfully complete the specific objectives set forth in the Collaborative Agreement. This additional funding request was granted by the FDA and was awarded on February 10, 2024. The additional funding is being used to fully complete the characterization of the reference cigarillo (1RSC) and filtered cigar (1RFC) products by contracting with two ISO 17025 accredited laboratories (Labstat and MSL) to conduct analyses to generate a new dataset for each reference cigar product. The labs will follow the CTRP protocol for the physical measurements and chemical analyses based

on the requirements and list of HPHCs set forth in the Collaborative Agreement at a cost of $334,213, and the overhead expenses required by UK federal contracting guidelines are $150,396.

- The main achievements for this reporting period include: (1) completing the 1RLC CoA and listing the product for sale on the CTRP website; (2) securing additional funding from the FDA in the amount of $484,609 to complete the characterization of the 1RSC and 1RFC; (3) substantial progress in the characterization of the 1RSC and 1RFC by Labstat and MSL; (4) additional internal preliminary analysis of constituents for the 1RLC, 1RSC, and 1RFC; (5) continuation of long-term stability studies on the previously manufactured non-certified CTRP reference cigars and the new certified reference cigars: 1RLC, 1RSC and 1RFC; and (6) toxicological research on reference and commercial cigar products.

I would like to thank Mr. Matthew Craft, Dr. Colin Fisher and Dr. Ruth McNees for their help with writing some sections of this report, and Dr. Colin Fisher, Dr. David Zaitlin and Ms. Cindy Stidham for their help with the compilation.

The KTRDC Quarterly Reports include copies and brief summaries of work published by KTRDC scientists and scientists partly funded by KTRDC, as well as work arising from KTRDC summit grants. I would like to thank Dr. Colin Fisher and Dr. Sitakanta Pattanaik for their help with writing the summaries. Names in bold indicate KTRDC or KTRDC-supported scientists.

Summary of Selected Research Topics

Report #1 "*Management of* Pythium myriotylum *in burley tobacco transplants and its effect on field productivity.*" **Robert Pearce**, William Barlow and Emily Pfeufer

This paper describes the experiments done to test the efficacy of chemicals to control pythium root rot in tobacco float beds and the effect of pythium on yield. Currently there is only one fungicide and one disinfectant registered in the US to control this disease, but another fungicide that is used for blue mold control could potentially also be effective. Both fungicides reduced the levels of pythium infection so that a greater proportion of plants survived in the field. This translated to an increase in yield of about 180 lb/acre.

Tobacco seedling production in float beds has many advantages over the outdoor bed method, but one of the disadvantages is that pythium root rot can cause a considerable loss of transplantable seedlings. The only chemicals registered in the US to control this disease are Terramaster (fungicide) and Oxidate (disinfectant). Some growers have, however, used Ridomil, normally used to control blue mold and black shank (both caused by oomycetes, like pythium). They claim that it worked well and did not burn the roots. The effect of this disease on crop yield has never been quantified, so this series of experiments set out to test the efficacy of these three chemicals and to quantify the effect of the disease on yield. The test was repeated each year for three years and although the timing of the chemical applications varied, each of the chemicals was tested with and without inoculating the float beds with the fungus. The effect of the disease on the health of the roots was measured using a visual scale of root damage and then counts of survivors in the field and the final yield. There were very few, if any, statistical differences between the chemical treatments or even between the treatments and the untreated check in any one year, except in one year when Ridomil significantly reduced the root damage. However, when the data for all three years were combined, both Terramaster and Ridomil reduced the disease severity. The establishment of seedlings in the first weeks after setting and survival through the season correlated with the severity of the root damage at setting. Overall, pythium-infected transplants reduced the saleable yield by about 180 lb./acre and in the current economic scope of tobacco production, this reduced yield will severely impact the profitability of the crop.

Report #2 *"Differential oxidative stress homeostasis in two burley tobacco varieties is linked to different peroxisomal glycolate oxidase levels."* Jasmina Kurepa and **Jan A. Smalle**

This research deals with metabolomics analyses of two burley tobacco varieties (KT204LC and NCBH 129LC) that differ significantly in tolerance to oxidative stress and TSNA accumulation. This research has identified factors responsible for differences in tolerance to oxidative stress between the two varieties, and attempts to correlate oxidative stress with TSNA accumulation. The abundance of oxidative stress markers (metabolites) is higher in the stress-tolerant variety (NCBH 129LC) compared to the sensitive one (KT204LC). The knowledge gained from this study

opens up possibilities for potential interventions to mitigate TSNA accumulation in burley tobacco during curing.

Tobacco-specific nitrosamines (TSNAs) are carcinogenic metabolites that accumulate in tobacco leaves during curing. One of the major objectives of the tobacco industry is to reduce the TSNA levels in tobacco products to address potential health concerns. TSNA levels in tobacco products depend on several factors such as tobacco type, growth conditions, nitrogen fertilizer, nicotine conversion, storage and curing conditions. A previous study has shown that the total alkaloid and nitrogen contents of two burley tobacco varieties, KT204LC and NCBH 129LC are similar; however, TSNA accumulation is significantly higher in NCBH 129LC compared to KT204LC. Additionally, NCBH 129LC shows relatively high tolerance to oxidative stress and accumulates more hydrogen peroxide (reactive oxygen species; ROS) compared to KT204LC. To identify the factors responsible for the differential response of these two tobacco varieties to oxidative stress, metabolomics analyses of leaves were performed. Metabolomics analyses revealed that the abundance of oxidative stress-responsive markers (metabolites) was significantly higher in the tolerant variety (NCBH 129LC) compared to the sensitive one (KT204LC). Additionally, the level of glycolate oxidase, a key enzyme responsible for production of hydrogen peroxide, was higher in NCBH 129LC compared to KT204LC. Elevated oxidative stress has been implicated in the formation of nitrosamines in animals, including humans. Thus, it would be interesting to investigate whether glycolate oxidase activity and hydrogen peroxide accumulation is linked to TSNA accumulation. This will open up new possibilities for potential interventions to mitigate TSNA accumulation in burley tobacco during curing.

Crop Protection 165 (2023) 106152

Contents lists available at ScienceDirect

Crop Protection

journal homepage: www.elsevier.com/locate/cropro

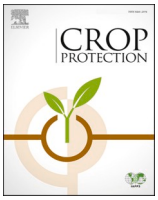

Management of *Pythium myriotylum* in burley tobacco transplants and its effect on field productivity

Robert Pearce [a], William Barlow [b], Emily Pfeufer [c,*]

[a] Department of Plant and Soil Sciences, University of Kentucky, Lexington, KY, 40546, USA
[b] Department of Plant Pathology, University of Kentucky, Lexington, KY, 40546, USA
[c] USDA ARS Foreign Disease Weed Science Research Unit, Ft. Detrick, MD, 21702, USA

A B S T R A C T

Pythium root rot (PRR) is a significant disease of tobacco transplants produced in the greenhouse floatbed system, but little is known about its influence once PRR-infected plants are transplanted in the field. Tobacco producers have limited chemical options to manage PRR, and additional data are needed on the efficacy of the fungicide active ingredients etridiazole, mefenoxam, and hydrogen peroxide-peroxyacetic acid. With the support of a pictorial, ordinal root ball quality (RBQ) rating scale, etridiazole and mefenoxam improved RBQ in tobacco transplants inoculated with *Pythium myriotylum* in greenhouse trials. In multi-year, generalized linear mixed model analyses, higher average RBQ in transplants significantly increased plant establishment, survival to season-end, and cured yield in research farm trials. To further apply the pictorial scale, a potential threshold of average RBQ >3.0 would be expected to result in 201 kg/ha more cured yield, over transplants with average RBQ ≤3.0. These results document for the first time the influence of transplant PRR on cured tobacco yield, in addition to its interim effects on tobacco establishment and survival. While additional data are needed to support a critical RBQ value, estimated effects of transplant quality on cured tobacco yield may assist growers in post-transplant farm management decisions, such as labor planning.

1. Introduction

Many different species of *Pythium* are capable of inducing disease symptoms, including pre- and post-emergent damping off, chlorosis, stunting, and most typically, root rot on numerous different types of plants (Krasnow and Hausbeck, 2017; Lookabaugh et al., 2015; Moorman et al., 2002; Rey et al., 1997; Schwarz et al., 2010; Zhang et al., 2021). Pythium root rot (PRR) is one of the most common diseases in tobacco (*Nicotiana tabacum* L.) transplant production, which primarily occurs in unique greenhouse conditions in the U.S. (Gutierrez et al., 2012; Zhang, 2021; Zhang et al., 2021). Most commercial growers using this system grow tobacco from seed to transplant in expanded polystyrene (EPS) trays filled with soilless planting medium and floated on shallow water containing dissolved fertilizer and pesticides. This occurs in custom-sized bays lined with black plastic film, utilizing retractable greenhouse curtains for heat and humidity management (Burley and Dark Tobacco Production Guide, 2021; Fortnum et al., 2000; Zhang et al., 2021). While the floatbed system eases some production constraints and generates consistent, high quality transplants in the absence of disease pressure, constantly submerged roots create favorable conditions for the development of PRR (Gutierrez et al., 2012; Zhang et al., 2021).

PRR in tobacco transplants is characterized by necrotic, slimy roots accompanied by chlorotic foliage, and is followed by sunken stem lesions and plant death in severe cases; up to 70% transplant loss has been reported due to PRR (Sigobodhla et al., 2010). PRR in tobacco floatbed systems has been associated with at least 12 different species of *Pythium,* with *P. myriotylum* Drechsler consistently reported as an aggressive species (Gutierrez et al., 2012; Mufunda et al., 2017; Zhang, 2021). While tobacco transplants with severe PRR have been reported as unusable, it was also noted that the overall impact on marketable tobacco yields from PRR-infected transplants is difficult to quantify (Gutierrez et al., 2012; Sigobodhla et al., 2010).

Few fungicides are labeled for management of PRR in the greenhouse by the U.S. Environmental Protection Agency (EPA; Gutierrez et al., 2012; Zhang, 2021; Zhang et al., 2021). U.S. EPA-labeled options include etridiazole (Terramaster 4 EC) and hydrogen peroxide combined with peroxyacetic acid (Oxidate 2.0); the former has been labeled for many years while the latter has been explored recently as an OMRI-listed option. Additionally, some tobacco growers have reported using a fungicide, mefenoxam, not labeled for this specific use (Pfeufer and Pearce, unpublished). To our knowledge, no efficacy data for hydrogen peroxide + peroxyacetic acid are available for tobacco floatbed systems. In comparisons of etridiazole and mefenoxam (Ridomil Gold SL),

* Corresponding author.
E-mail address: Emily.Pfeufer@usda.gov (E. Pfeufer).

https://doi.org/10.1016/j.cropro.2022.106152
Received 11 May 2022; Received in revised form 14 November 2022; Accepted 15 November 2022
Available online 25 November 2022
0261-2194/Published by Elsevier Ltd.

Gutierrez et al. (2012) found etridiazole managed PRR more effectively, while Zhang et al. (2021) found mefenoxam managed PRR more effectively; both studies utilized *P. myriotylum* to induce PRR. In addition to a dearth of labeled options for this pathosystem, other major reasons growers explore alternate fungicides are the occurrences of stunting and/or seedling loss when etridiazole is applied too early in the production season (Zhang et al., 2021) and/or if incorporated non-uniformly (Gutierrez et al., 2012; Terramaster 4 EC product label).

To improve our understanding of the impact of Pythium root rot (PRR) on tobacco production, we hypothesized that 1) tobacco transplant RBQ as influenced by PRR would be affected by the choice of fungicide in float water; and 2) PRR-influenced transplant RBQ affects tobacco establishment, survival, and cured yield. To test these hypotheses, we used data derived from an ordinal tobacco root ball quality (RBQ) scale, supported by photos and written descriptions. Similar scales have been used in other evaluations of PRR (Fortnum et al., 2000; Zhang et al., 2021), but to our knowledge pictorial support was not made available. After future experimentation, it is our hope that this pictorial scale will be utilized by growers for data-supported production planning.

2. Materials and methods

2.1. Transplant production

From 2016 to 2018, burley tobacco plants were produced in grower-standard, 288-cell expanded polystyrene (EPS) trays in large beds segregated into eight experimental units. Each experimental unit was lined with black plastic for water retention and water was not shared among the units, which were maintained evenly at 60.6 L water volume throughout the experimental period. Each unit was subjected to a single fungicide treatment (or untreated control) and was either inoculated or noninoculated a single time. Fungicide treatments were etridiazole (Terramaster 4 EC, Chemtura, Middlebury, CT), mefenoxam (Ridomil Gold SL, Syngenta Crop Protection, Greensboro, NC), hydrogen peroxide-peroxyacetic acid (Oxidate 2.0, Biosafe Systems, East Hartford, CT), or a nontreated control. The large bed containing eight units was considered the blocking factor in each experiment; 2016 had three blocks (experimental replicates) while 2017 and 2018 trials had four. This resulted in a sample size of 11 for each fungicide-*P. myriotylum* combination in the transplant evaluation analyses.

Trays were filled with Carolina Choice Tobacco Mix (Carolina Soil Company, Kinston, NC) and seeded with 'TN-90LC' and 'KT-212LC' seed in 2016–2017 and 2018 trials, respectively. Tobacco varieties have not been found to differ in susceptibility to *P. myriotylum* (Sigobodhla et al., 2010). Plants were fertilized weekly with 20-10-20 NPK fertilizer to a maintenance EC of approximately 1.0 mS/cm. Seedlings were grown to the size of typical transplant by growers, approximately 0.75 cm stem diameter. Plants were clipped weekly with a mower suspended approximately 6 cm above the plant buds and treated with Orthene 97 (0.82 g/L, over approximately 30.9 m^2 of floatbed; Amvac Chemical Corp., Newport Beach, CA) for aphid and other insect management, per grower standard practice. For target spot and other foliar disease management, mancozeb (Manzate ProStick; 0.6 g/L; applied to foliar coverage) was applied weekly beginning at canopy closure, with one application of azoxystrobin (Quadris Flowable; 4 ml/92.9 m^2) immediately following the first clipping. The three trials were conducted on university research farm in fields without histories of other soilborne diseases. Experimental dates are included in Table 1.

2.2. Pythium myriotylum inoculation and disease management

Experimental units were inoculated in each of the three trials with *Pythium myriotylum* isolate 16-PmDn, which was locally derived in 2016 from an infected tobacco transplant and maintained on clarified V8 (CV8) medium throughout the studies. The isolate was established by aseptically transferring a hyphal tip to CV8 medium. Species identity was confirmed by PCR amplification of *coxI* using the primers OomCoxI-Levup and Fm85mod (Robideau et al., 2011), followed by bidirectional Sanger-sequencing (Eurofins Genomics, Louisville, KY) of the 718-bp amplicon, which was used as input to NCBI's Blast tool. The isolate was 100% identical (718/718 bp) to *P. myriotylum* NCBI Genbank accession MT222755 as well as 100% identical to multiple *P. myriotylum* voucher specimens (at 91% or greater coverage), including CBS25470 (Genbank accession HQ708745); the top 100+ Genbank BLAST results indicated best matches to *P. myriotylum*. Approximately 7-day old cultures (± 2 days) of *P. myriotylum* 16-PmDn were established on CV8 medium prior to inoculation each trial year. A #3 cork borer (interior diameter 5 mm) was used to remove uniformly colonized agar plugs of mycelium from the leading edge of the colony plates. Four colonized agar plugs were added to the water where transplant trays were floating, one in the middle of each of the four sides of inoculated experimental units. Inoculation took place after plant roots had grown into the water, which commonly occurs in this production system.

2.3. Root ball quality ratings

A root ball quality (RBQ) rating scale was developed for burley tobacco transplants grown in the floatbed system (Fig. 1). The scale encompasses the degree of necrosis occurring on the root ball (due to inoculation with *P. myriotylum* or phytotoxic effects of the fungicides), root softness, and the degree of root colonization within the media in the cell. The RBQ scale ranged from 0 to 5, with 0 describing a completely brown/black root ball with nearly complete softness of lower roots and a less than 50% full cell. Cell fullness encompasses roots visibly colonizing the media as well as the plug being removed intact; in cases where plants were heavily affected by root rot, the media fell away from the plug. Heavily necrotic roots that were not macroscopically visible within the plug would also be considered in the cell fullness portion of the rating. A rating of 1 described a rootball with more than 80% necrotic roots, a

Table 1
Experimental details by trial year examining influence of *Pythium myriotylum* and fungicides in transplant float bed systems on field tobacco production, conducted from 2016 to 2018 in Kentucky.

Year	Seeding date	Inoculation date	Treatment date	Days from inoculation to treatment	Rootball evaluation	Transplant date	Harvest date	Data collected
2016	5/13	6/3	6/3	0 days	6/22	6/24	9/26	RBQ[z], Survival[y], Cured yield[x]
2017	2/12	6/2	6/12	10 days	6/26	6/27	9/28	RBQ, Establishment[w], Survival, Cured yield
2018	4/17	6/11	6/16	5 days	6/25	7/2	10/2	RBQ, Establishment, Survival, Cured yield

[z] Average root ball quality rating using the scale in Fig. 1 on 10 randomly selected plants per experimental unit (tray).
[y] Survival is the presence of plants in plot counts within 3 weeks of harvest, as a percentage of the total number of originally placed transplants per plot.
[x] Cured yield per hectare, following grower-standard curing practices for approximately 3 months after harvest and assuming a 792 plant/hectare population.
[w] Establishment is defined as the presence of transplants in plot counts 2–3 weeks after transplanting, as a percentage of the total number of originally placed transplants per plot.

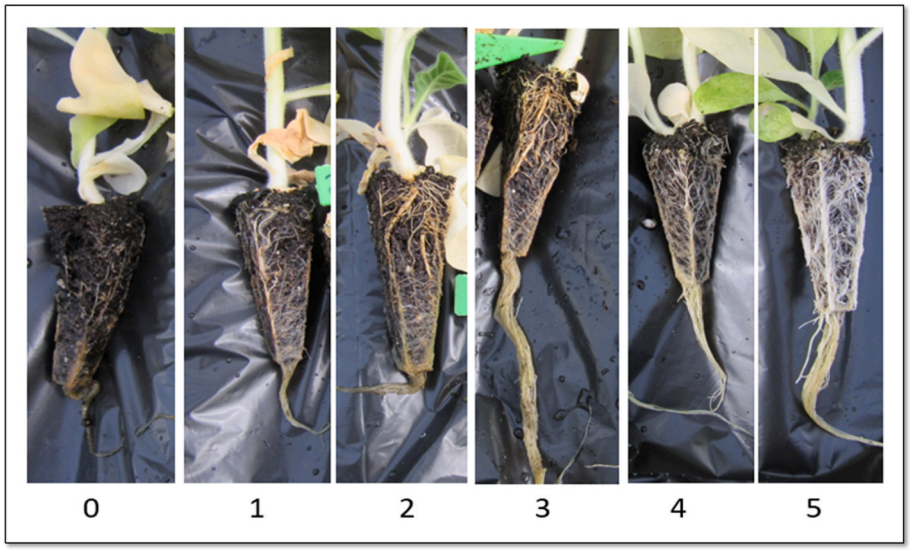

Fig. 1. Ordinal (0–5) root ball quality (RBQ) scale for burley tobacco transplants produced in the float-bed system with Pythium root rot pressure from *Pythium myriotylum*. The RBQ scale ranged from 0 to 5, with 0 describing a completely brown/black root ball with nearly complete softness of lower roots and a less than 50% full cell. A rating of 1 described a rootball with more than 80% necrotic tissue, a 50–75% full cell, and over 50% soft roots. A rating of 2 described a 60–80% necrotic root ball in an over 75% full cell, with approximately 50% soft roots. A rating of 3 described a 40–60% necrotic rootball, in an over 75% full cell, with 25–50% root softness. No softness was present at ratings at and above 4. A rating of 4 described a 10–40% necrotic rootball in an over 75% full cell. A rating of 5 described a nearly completely white rootball that completely filled the cell. (For interpretation of the references to colour in this figure legend, the reader is referred to the Web version of this article.)

50–75% full cell, and over 50% soft roots. A rating of 2 described a 60–80% necrotic root ball in an over 75% full cell, with approximately 50% soft roots. A rating of 3 described a 40–60% necrotic rootball, in an over 75% full cell, with 25–50% root softness. No softness was present at ratings at and above 4, and in the few cases where a transplant fell between ratings, the softness portion of the rating took precedence. A rating of 4 described a 10–40% necrotic rootball in an over 75% full cell. A rating of 5 described a nearly completely white rootball that completely filled the cell. Ten randomly selected transplants per 288-cell tray were visually rated to estimate RBQ for the entire tray up to 7 days prior to transplanting; rated plants were not taken to the field but remaining plants from the same tray were used to establish each field replicate. Rating a tray sample of 10 plants took approximately 10 min, including photodocumentation. Three (2016) or four replicates were rated for each experimental treatment (inoculated/noninoculated x fungicide) per year, with each greenhouse replicate corresponding directly to a field replicate, resulting in experimental n = 88 and inoculation x fungicide n = 11, across three trials.

2.4. Fungicides and application intervals

Three fungicidal treatments (etridiazole, mefenoxam, hydrogen peroxide-peroxyacetic acid) were utilized along with a nontreated control. Inoculated and noninoculated units were treated with fungicides, for a total of 8 inoculation x fungicide treatments in these trials. Four (2017–2018) or three (2016) experimental replicates of each treatment were included in each trial in a randomized complete block design in both the greenhouse and the field. Etridiazole (0.055 ml/L) was utilized as the 'grower standard' fungicide. Mefenoxam (0.011 ml/L) was an alternative, albeit unlabeled by U.S. EPA, fungicide. The mefenoxam concentration was suggested by a grower with extended experience using the product in this manner. Hydrogen peroxide-peroxyacetic acid (1:5000 v/v) was also tested. Fungicides were added to water in multiple areas of each experimental unit, then additional fresh water was added in these same areas to normalize the volume of each section to 60.6 L, while also circulating fungicide. Trays were gently agitated to promote complete mixing of fungicide. The timing of fungicide treatment relative to inoculation was 0 days post inoculation (dpi), 10 dpi, and 5 dpi, in 2016, 2017, and 2018, respectively. Chlorotic foliar symptoms in untreated trays generally appeared 8–10 dpi. Experimental replicate volume was checked multiple times per week and maintained at 60.6L as plants continued to grow.

2.5. Field production and data collection

Tobacco transplants were placed in fields in a randomized complete block design with four (three in 2016) replications of each fungicide-inoculation combination (eight total "treatments" in each trial). Initial plot size varied between 24 and 28 plants by year in double-row plots with 0.53 m in-row spacing and 1.07 m between row spacing as established with a mechanical tobacco transplanter. Plots received typical agronomic management, including cultivation, topping, and sucker control, without in-field fungicide applications (Burley and Dark Tobacco Production Guide, 2021). In all trials, an approximate 1.5 m plant-free break was included between experimental plots.

Plants were counted in each plot at transplanting, two to three weeks after transplanting, and after approximately three months in the field, approximating a typical burley tobacco crop cycle. At harvest, plants were cut near the base of the stem and speared on tobacco sticks labeled with the plot number. After 2–3 days of wilting in the field, labeled sticks were hung in a tobacco barn to be air-cured in ambient conditions for approximately 12 weeks. After the curing process, leaves were stripped from the stalks, sorted, and weighed. The number of plants surviving two to three weeks after transplanting was calculated as a percentage of the plants transplanted and is referred to as establishment. The number of plants surviving three or more months after transplanting was calculated as a percentage of the plants transplanted and is referred to as survival. Yield was determined on a per-plot basis by calculating the weight of cured tobacco per plot divided by the number of plants transplanted per plot, then multiplying by 17,792, a typical per-hectare burley tobacco plant population. An experimental plot constitutes a sample in all analyses presented.

2.6. Statistical analyses

Descriptive statistics for root ball quality (RBQ), establishment, survival, and cured yield were generated in SAS 9.4 (SAS Institute Inc., Cary, NC). Correlations were completed on raw dependent variables using Minitab 19 (State College PA, USA). The influence of *P. myriotylum* inoculation on establishment, survival, and cured yield was evaluated using General Linear Model in Minitab 19; experimental replicate (a blocking factor) was included as a random variable nested in year, a fixed factor.

2.6.1. Greenhouse floatbed fungicide effects on tobacco root ball quality ratings, establishment, survival, and cured yields

To compare the effects of various greenhouse floatbed water fungicide treatments to respective nontreated controls, nonparametric and parametric tests were executed. One tray represented a replicate in each experimental year, which was transplanted into a corresponding field replicate; n = 11 for each fungicide-inoculation combination, divided among three experimental years (Table 2). A combined-year Kruskal Wallis test was used to compare median RBQ ratings within inoculation status, and pairwise Mann-Whitney tests were applied between the respective nontreated control and floatbed fungicide treatment RBQ medians using Minitab 19.

Generalized linear mixed model analyses (GLMMs) were applied using PROC GLIMMIX in SAS 9.4 (Cary NC, USA) to determine the effects of the binary variable *P. myriotylum* 16-PmDn inoculation and the class variable floatbed fungicide on tobacco establishment, survival, and cured yield. Experimental replicate (a random blocking factor) nested in the fixed factor, experimental year, was included in the combined analysis. After inspection of model residuals, establishment and survival proportions were arcsin ($\sqrt{y}$)-transformed based on improvements to the assumption of normality in the analysis residuals (Zhang et al., 2021). Least squares means of the combined-year analysis were

Table 2
Descriptive statistics, Kruskal-Wallis and Mann-Whitney tests on median tobacco rootball quality (RBQ), and least squares means from generalized linear mixed model analyses relating fungicide and inoculation status to establishment, survival, and cured yield, from greenhouse-to-field trials conducted in Kentucky and separated by year (2016–2018).

2016		RBQ[z] descriptive statistics				Median RBQ compared by treatment within inoculation		Least squares means on fungicide x 16-PmDn inoculation interaction[y]		
Fungicide	Inoculated (16-PmDn)	Min	Max	Mean	Median	K-W[x] *P* value	M-W *P* value[w]	Establish.[v]	Survival[u]	Cured yield (kg/ha)[t]
HP + PAA[s]	No	2.9	4.8	4.0	4.3	.	1.000	.	89.9	3514
Mefenoxam[r]	No	2.8	4.1	3.4	3.2	.	0.190	.	87.3	3372
Etridiazole[q]	No	4.5	4.9	4.7	4.8	.	0.190	.	87.3	3350
NTC[p]	No	3.3	4.6	4.1	4.4	0.099	.	.	91.0	3563
Etridiazole	Yes	4.5	4.9	4.7	4.8	.	0.081	.	87.4	2982
HP + PAA	Yes	3.8	4.5	4.2	4.4	.	0.081	.	91.0	2821
NTC	Yes	0.0	1.4	0.7	0.8	0.037	.	.	91.8	2814
Mefenoxam	Yes	3.5	4.6	3.9	3.6	.	0.081	.	90.0	2636
2017		**RBQ[z] descriptive statistics**				**Median RBQ compared by treatment within inoculation**		**Least squares means on fungicide x 16-PmDn inoculation interaction[y]**		
Fungicide	Inoculated (16-PmDn)	Min	Max	Mean	Median	K-W[x] *P* value	M-W *P* value[w]	Establish.[v]	Survival[u]	Cured yield (kg/ha)[t]
HP + PAA[s]	No	4.5	4.8	4.7	4.7	.	0.372	97.9	97.9	2810
Mefenoxam[r]	No	3.7	5.0	4.4	4.4	.	1.000	98.5	96.9	2933
Etridiazole[q]	No	4.3	5.0	4.6	4.7	.	0.384	96.9	96.9	2604
NTC[p]	No	3.9	4.8	4.4	4.4	0.555	.	97.4	94.2	2495
Etridiazole	Yes	0.8	0.8	0.8	0.8	.	.[o]	96.1	93.1	2585
HP + PAA	Yes	0.3	0.9	0.7	0.8	.	0.661	97.6	93.9	2533
NTC	Yes	0.1	0.9	0.5	0.6	0.043	.	91.7	91.7	2673
Mefenoxam	Yes	0.9	2.0	1.3	1.2	.	0.055	92.7	91.6	2119
2018		**RBQ[z] descriptive statistics**				**Median RBQ compared by treatment within inoculation**		**Least squares means on fungicide x 16-PmDn inoculation interaction[y]**		
Fungicide	Inoculated (16-PmDn)	Min	Max	Mean	Median	K-W[x] *P* value	M-W *P* value[w]	Establish.[v]	Survival[u]	Cured yield (kg/ha)[t]
HP + PAA[s]	No	4.8	5.0	5.0	5.0	.	0.072	100 a	87.7	2080
Mefenoxam[r]	No	4.7	4.9	4.8	4.9	.	0.369	100 a	89.1	1935
Etridiazole[q]	No	4.8	5.0	4.9	4.8	.	0.353	96.8 ab	85.7	1980
NTC[p]	No	4.6	4.9	4.7	4.7	0.152	.	99.1 ab	85.6	1916
Etridiazole	Yes	1.6	3.3	2.7	2.9	.	0.112	99.1 ab	86.6	1784
HP + PAA	Yes	1.1	1.9	1.7	1.8	.	1.000	94.1 ab	84.1	1922
NTC	Yes	0.9	2.4	1.6	1.5	0.016	.	87.7 b	79.5	1731
Mefenoxam	Yes	3.3	4.2	3.8	3.8	.	0.030	100 a	85.0	2068

[z] Root ball quality ratings averaged from 10 random plants per experimental replicate, evaluated using scale in Fig. 1. Three and four experimental replicates were present in 2016 and 2017–2018, respectively.

[y] Least squares means from general linear mixed model analysis of variance on arcsin($\sqrt{y}$)-transformed establishment and survival, and untransformed cured yield by fungicide x *P. myriotylum* 16-PmDn inoculation ("treatment") using experimental replicate as a random variable. Statistically significant differences by column are indicated by different letters following treatment least squares means, as determined by a Tukey-Kramer post hoc test ($P < 0.05$).

[x] *P*-value from inoculation-wise, nonparametric Kruskal-Wallis test comparing median RBQs in the dataset, adjusted for ties.

[w] *P*-value from pairwise, nonparametric Mann-Whitney test comparing treatment median RBQ to respective nontreated control, adjusted for ties.

[v] Establishment is the number of plants in experimental field plots 2–3 weeks into the season as a percentage of the number of plants transplanted in the plot (2017 and 2018).

[u] Survival is the number of plants in experimental field plots approximately three months after transplant as a percentage of the number of plants transplanted in the plot.

[t] Cured yield is the weight (kg) of harvested tobacco leaves by experimental field plots after hanging in a barn for approximately 3 months after harvest with ambient temperature and humidity, divided by number of plants originally transplanted in the plot, then multiplied by a typical plant population of 17,792 plant/ha.

[s] Hydrogen peroxide + peroxyacetic acid, active ingredients in Oxidate 2.0.

[r] Active ingredient in Ridomil Gold SL.

[q] Active ingredient in Terramaster 4 EC.

[p] Nontreated control.

[o] All RBQ ratings were 0.8 resulting in no variability, so comparison was not possible.

requested using the Tukey-Kramer adjustment with statistically significant differences indicated by $P < 0.05$.

2.6.2. Root ball quality effects on establishment, survival, and cured yields

GLMMs were completed on individual trial year datasets (n = 24 or 32), combined-year datasets subsetted by *P. myriotylum* inoculation status (n = 44), and the full dataset (n = 88) using average RBQ per tray as a predictor of establishment, survival, and cured yield. Experimental replicate was included as a random variable in the trial year models, while experimental replicate nested in year was a random variable in the combined-year models. Establishment and survival were arcsin ($\sqrt{y}$)-transformed based on improvements to the assumption of normality in the analysis residuals (Zhang et al., 2021). Type III Fixed Effect *P* values using the predictors 16-PmDn inoculation, fungicide used in the floatbed, and their interaction are reported for each dependent variable in the trial year analyses. In all statistical analyses, significance was indicated by $P < 0.05$. In analyses where average RBQ was a statistically significant predictor, the effect of a one-unit change was estimated assuming a typical plant population of 17,792 plants/ha.

2.6.3. Example threshold RBQ on cured yield

To suggest one potential application of the RBQ scale by growers, PROC GLIMMIX was used to compare experimental plots grouped by the independent variable average RBQ in regard to their cured marketable yields. As in other analyses, experimental replicate nested in year was included as a random variable and a sample was an experimental plot (n = 88). A critical value of 3.0 was assumed for average RBQ, resulting in comparison of two experimental groups (RBQ ≤3.0; RBQ >3.0), using a Tukey-Kramer post-hoc test ($P < 0.05$). PROC SGPLOT was used to construct the scatter diagram in Fig. 2.

3. Results

3.1. Greenhouse fungicide effects on tobacco root ball quality

Root ball quality (RBQ) was utilized to measure root necrosis, softness, and the fullness of the tobacco transplant root ball filling the tray cells following inoculation with *P. myriotylum* 16-PmDn and management with etridiazole, mefenoxam, or hydrogen peroxide + peroxyacetic acid. Using the scale in Fig. 1, ratings were applied to ten transplants and averaged to represent RBQ for the experimental replicate. When results were considered year-by-year, experiment-wide differences in median RBQ were apparent in inoculated plants in every year (Table 2). However, when fungicide treated plants were individually compared to the inoculated nontreated control within each year, the only statistically significant difference at α = 0.05 occurred between mefenoxam-treated inoculated plants and nontreated inoculated plants in 2018 (Table 2).

When trial year data were combined, the three-trial median RBQ for inoculated mefenoxam- (3.4) and etridiazole-treated (2.8) plants was significantly higher than inoculated, nontreated plants (0.9; $P \leq 0.025$). In noninoculated plants, no statistically significant differences in median RBQ were apparent among treatments and the nontreated control, suggesting no phytotoxic fungicide effects were present in these trials (Table 3).

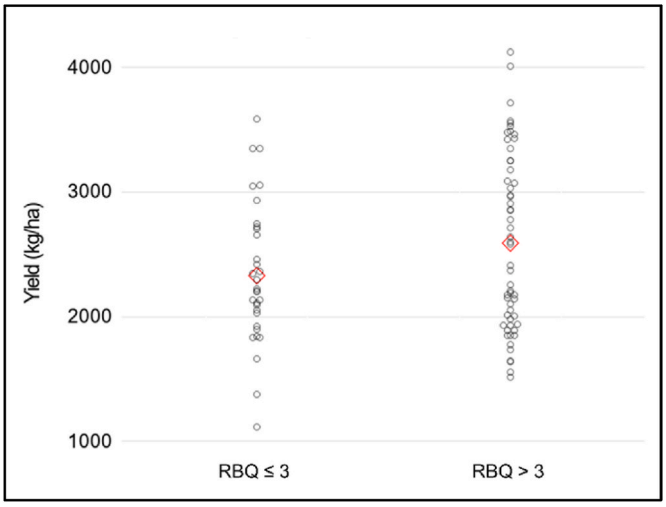

Fig. 2. Cured burley tobacco yields compared between experimental plots with *P. myriotylum*-influenced RBQ ≤3.0 or RBQ >3.0. Circles indicate individual experimental plots, while the diamond in each column indicates the least-squares mean of the experimental group. The RBQ >3.0 group mean of 2571 kg/ha was significantly greater than the RBQ ≤3.0 group mean, 2370 kg/ha (PROC GLIMMIX followed by Tukey-Kramer comparison, $P = 0.026$).

3.2. Greenhouse fungicide and P. myriotylum inoculation effects on tobacco establishment, survival, and cured yield

When the raw dependent variables tobacco establishment, survival, and cured yield were compared, establishment was positively correlated with survival ($P < 0.001$) and survival was positively correlated with cured yield ($P < 0.001$), though no direct correlation between establishment and cured yield was present (Table S1). In single-year trials, only one statistically significant difference was indicated within inoculation status, whereby inoculated, mefenoxam-treated plants established significantly better than inoculated, nontreated plants (Table 2). In the combined-year dataset, only a few differences were apparent, none of which occurred in plants of the same inoculation status. The most notable was that noninoculated mefenoxam-treated plants resulted in significantly higher cured yield than inoculated mefenoxam-treated plants ($P < 0.05$; Table 3). Using a Kruskal-Wallis analysis, median RBQ values did not differ when noninoculated controls were compared among trial years. Similarly, median RBQ for inoculated, nontreated controls did not differ among trial years, despite differences in the inoculation to treatment timelines ($P > 0.05$; data in Table 2 and Fig. S; analysis not shown).

Combining all floatbed fungicide treatments (including nontreated) and years, inoculation with *P. myriotylum* reduced establishment from 96.5% to 93.1% ($P = 0.046$) and cured yield from 2698 kg/ha to 2403 kg/ha ($P < 0.001$; data shown by treatment and trial year in Table 2). GLMMs were completed using *P. myriotylum* inoculation status, floatbed fungicide used, and their interaction in modeling tobacco establishment, survival, and cured yield in standalone trial years. Inoculation with *P. myriotylum* 16-PmDn significantly reduced tobacco establishment in the 2017 ($P = 0.0330$) and 2018 ($P = 0.0335$) trials. Inoculation with 16-PmDn also significantly reduced tobacco survival in the 2017 trial ($P = 0.0423$) and cured yield in the 2016 trial ($P = 0.0070$; Table S2).

3.3. Relationships between average RBQ and establishment, survival, and cured tobacco yield

Since no statistically significant differences were apparent in establishment, survival, or cured yield among fungicide treatments without including the *P. myriotylum* 16-PmDn inoculation status predictor, GLMMs were applied to data separated by inoculation status (n = 32 or 44) as well as the full dataset (n = 88) in regard to the influence of average RBQ. In inoculated plants only, average RBQ was a statistically significant predictor of tobacco plant establishment ($P = 0.0022$), however, it was not associated with survival or cured yield in inoculated plants nor in any of the noninoculated analyses (Table S3). In the full dataset, with a larger sample size and encompassing both inoculated and noninoculated plants, average RBQ was a positive predictor of establishment ($P = 0.0002$), survival ($P = 0.0055$), and cured yield ($P = 0.0178$; Table 4). To further simplify the use of the scale and present one way growers may independently apply it on their farms, experimental

Table 3
Descriptive statistics, Kruskal-Wallis and Mann-Whitney tests on median tobacco rootball quality (RBQ), and least squares means from generalized linear mixed model analyses relating fungicide and status of *Pythium myriotylum* inoculation to establishment, survival, and cured yield, from greenhouse-to-field trials conducted in Kentucky (2016–2018).

Fungicide	Inoculated (16-PmDn)	RBQ[z] descriptive statistics				Median RBQ compared by treatment within inoculation		Least squares means on fungicide x 16-PmDn inoculation interaction[y]		
		Min	Max	Mean	Median	K-W[x] *P* value	M-W *P* value[w]	Establish.[v]	Survival[u]	Cured yield (kg/ha)[t]
HP + PAA[s]	No	2.9	5.0	4.6	4.8	.	0.184	99.5 a	92.8	2736 a
Mefenoxam[r]	No	2.8	5.0	4.3	4.4	.	0.948	99.6 a	92.0	2690 a
Etridiazole[q]	No	4.5	5.0	4.7	4.8	.	0.070	96.8 ab	91.0	2580 ab
NTC[p]	No	3.3	4.9	4.4	4.6	0.216	.	98.3 a	90.5	2576 ab
Etridiazole	Yes	0.8	4.9	2.5	2.8	.	0.025	97.9 ab	89.3	2402 ab
HP + PAA	Yes	0.3	4.5	2.0	1.7	.	0.114	96.1 ab	89.9	2389 ab
NTC	Yes	0.4	2.4	1.0	0.9	0.017	.	89.8 b	87.8	2369 ab
Mefenoxam	Yes	0.9	4.6	2.9	3.4	.	0.002	98.2 ab	88.9	2241 b

[z] Root ball quality ratings averaged from 10 random plants per experimental replicate, evaluated using scale in Fig. 1. Three and four experimental replicates were present in 2016 and 2017–2018, respectively, for a total n = 11 for each row and a grand total n = 88.

[y] Least squares means from general linear mixed model analysis of variance on arcsin($\sqrt{y}$)-transformed establishment and survival, and untransformed cured yield by fungicide x *P. myriotylum* 16-PmDn inoculation ("treatment") using experimental replicate nested in year as a random variable. Statistically significant differences by column are indicated by different letters following treatment least squares means, as determined by a Tukey-Kramer post hoc test ($P < 0.05$).

[x] *P*-value from inoculation-wise, nonparametric Kruskal-Wallis test comparing treatment median RBQ to respective nontreated control, adjusted for ties.

[w] *P*-value from pairwise, nonparametric Mann-Whitney test comparing treatment median RBQ to respective nontreated control, adjusted for ties.

[v] Establishment is the number of plants in experimental field plots 2–3 weeks into the season as a percentage of the number of plants transplanted in the plot (2017 and 2018).

[u] Survival is the number of plants in experimental field plots approximately three months after transplant as a percentage of the number of plants transplanted in the plot (2016–2018).

[t] Cured yield is the weight (kg) of harvested tobacco leaves by experimental field plots after hanging in a barn approximately 3 months after harvest with ambient temperature and humidity, divided by number of plants originally transplanted in the plot, then multiplied by a typical plant population of 17,792 plant/ha (2016–2018).

[s] Hydrogen peroxide + peroxyacetic acid, active ingredients in Oxidate 2.0.

[r] Active ingredient in Ridomil Gold SL.

[q] Active ingredient in Terramaster 4 EC.

[p] Nontreated control.

plots grouped by average RBQ >3.0 had significantly higher cured burley tobacco yields (2571 kg/ha) as compared to plots with RBQ ≤3.0 (2370 kg/ha; $P = 0.026$; Fig. 2).

4. Discussion

The multi-year results presented here quantify for the first time how tobacco transplant root ball quality (RBQ), as influenced by *P. myriotylum* and potential phytotoxicity of fungicides in the floatbed system, relates to plant establishment, survival, and cured leaf yields (Tables 2 and 3). The magnitudes of the effect of a one-unit increase in RBQ, which ranged from 1.8% more surviving plants to 2.6% more cured yield (63.1 kg/ha from a target yield of 2466 kg/ha) to 3.7% more established plants, are relatively small in comparison to losses observed in other water-intensive production systems affected by *Pythium* spp., such as 12–54% yield loss in hydroponic lettuce (Stanghellini and Kronland, 1986), 5.8–28% in hydroponic tomato (Rey et al., 1997; Schwarz et al., 2010), and 32% in soilless cannabis production (McGehee and Raudales, 2021). However, when small RBQ effects are multiplied over 8 to 40 ha—the typical production size of burley tobacco operators in Kentucky—they become economically relevant to growers, who operate on increasingly constrained margins. The average price for cured burley tobacco has stagnated in KY in the last few decades, with 10-year averages of $4.09, $3.99, and $4.10 per kilogram in 2000, 2010, and 2020, respectively (USDA NASS United States Department of Agriculture National Agricultural Statistics Service Quickstats, 2022). During the same time period, however, nearly every production cost has increased, and one recent economic analysis suggested returns to operators as approximately $253/ha in 2021, as compared to approximately $2200/ha in 2003–2005 (Snell, 2021). Thus, a one-unit change in RBQ and its reduction in cured yield could result in annual production costs exceeding returns to growers.

Median RBQ in plants inoculated with *P. myriotylum* was improved when etridiazole or mefenoxam were used in transplant production floatbeds, using multi-year results combined into a single nonparametric analysis (Table 3). Previous evaluations with *P. myriotylum* from tobacco suggested PRR reductions using each of these fungicides (Gutierrez et al., 2012; Zhang et al., 2021), but varied in terms of the single most effective compound; no reproducible differences between the two products were identified here. As hypothesized by Zhang et al., results from product comparison studies may also vary due to experimental conditions, such as the inoculation method and time to treatment (2021). Our inoculation methods differed from previous evaluations in that we utilized uniformly colonized agar plugs as opposed to a pathogen slurry (Gutierrez et al., 2012; Zhang et al., 2021), and our time to treatment varied by each experimental trial year. Colonized agar plugs, as used in our trials, may more closely approximate how PRR naturally develops in the floatbed system – from localized foci where *Pythium* spp. are introduced into the bed, rather than uniformly incorporated, high-concentration inoculum. We attempted to ensure uniformity among experimental units by identical placement of colonized plugs at regular intervals in each experimental unit, and PRR disease pressure was consistently high among experimental years in the nontreated, inoculated controls. While the floatbed fungicide comparisons presented here compile three different durations between inoculation and treatment, we encourage additional replications of each time-to-treatment, in addition to replications at other tobacco transplant sites with alternate environmental conditions, especially temperature. Water temperature has been shown to affect tobacco PRR (Fortnum et al., 2000); in our study, the greenhouse heating and cooling was managed at 21 C, with heaters, vents, and fans automatically activated above and below that temperature. When conditions consistently exceeded 30 C during the day, greenhouse curtains were opened, similar to commercial growing conditions. Tobacco transplant crops were maintained in other beds in the same greenhouse and no indications of temperature stress were noted, however, water temperature was not specifically monitored

Table 4
Generalized linear mixed models of the arcsin ($\sqrt{y}$)-transformed dependent variables establishment and survival, and untransformed cured yield per hectare, described by average transplant root ball quality (RBQ), from tobacco trials inoculated with *Pythium myriotylum* and conducted in Kentucky (combined from 2016 to 2018).

Dependent variable	Factor [z]	Coefficient	t value	*P* value [y]	Estimated effect per hectare with one-unit change in average RBQ
Establishment [y]	Intercept	1.2975	30.29	<0.0001	.
	Avg RBQ[x]	0.03737	3.92	0.0002	+665 more established plants/ha
Survival [w]	Intercept	1.1966	32.03	<0.0001	.
	Avg RBQ	0.01762	2.86	0.0055	+313 more surviving plants/ha
Cured yield [v]	Intercept	2289.55	11.72	<0.0001	
	Avg RBQ	63.0708	2.09	0.0178	+63.1 more cured kg/ha

u Cured yield per hectare, following grower-standard curing practices for approximately 3 months and assuming a 17,792 plant/hectare population.

[z] Experimental replicate (block) was coded in each analysis as a random variable nested in trial year.

[y] Critical value is 0.05, as reported from Type III results.

[x] Establishment is defined as the presence of transplants in plot counts 2–3 weeks after transplanting, as a percentage of the total number of originally placed transplants per plot. This analysis includes the 2017–2018 datasets.

[w] Average root ball quality from 10 randomly rated plants by experimental replicate, using the scale in Fig. 1.

[v] Survival is the presence of plants in plot counts within 3 weeks of harvest, as a percentage of the total number of originally placed transplants per plot.

in our study. Other studies, from an ornamental system, suggested acidic conditions may improve etridiazole's efficacy against *Pythium* spp. in some cases (Krasnow and Hausbeck, 2017); this has never been explored in the tobacco floatbed system and may be another reason for variability in fungicide efficacy among research groups.

The analyses presented here demonstrate average RBQ as influenced by *P. myriotylum* inoculation is a statistically significant predictor of establishment, survival, and cured yield, despite broad variability among trial years due to season-specific environmental factors (see noninoculated, nontreated controls in Table 3 as an example) as well as time-to-treatment. By controlling for the effects of trial year in each GLM analysis, this suggests relationships with average RBQ may be present in spite of the growing and curing environment. Some examples of environmental conditions that may affect tobacco establishment and vary by year include post-transplant weather conditions, particularly precipitation, and field soil types, especially water-holding capacity and organic matter. Survival and yield, which occur 3 and 8 months after transplant, respectively, would be expected to diverge even more strongly from transplant effects due to the vastly larger number of events occurring in the field and during curing. That the effect of average RBQ influenced by *P. myriotylum* is consistently maintained over these dependent variables demonstrates that PRR management is worthwhile for tobacco growers. While fungicide treatments were administered at different intervals in each trial year, results from the combined dataset may reflect differences in how growers utilize fungicides in this system: some treat plants preventatively, while others may wait for symptom development. Both etridiazole and mefenoxam were robust in managing PRR in tobacco transplant production using this range of application timelines. As the average RBQ relationship is replicated in future work, the number of experimental replicates in a given year should be increased to improve the predictive capability of a single trial year dataset.

To further improve the visual RBQ scale's applicability to commercial growers, one potential threshold of average transplant RBQ was explored in regard to cured tobacco yields. In this case, transplants with RBQ >3.0 averaged an additional 201 kg/ha of cured yield, significantly greater than plots with RBQ ≤3.0 (Fig. 2). Price received per kilogram of cured burley tobacco varies annually based on a number of factors, however, the 10-year average price in 2020 was $4.10 USD/kg (USDA NASS United States Department of AgricultureNational Agricultural Statistics Service Quickstats, 2022). Using this figure, the impact of average transplant RBQ ≤3.0 is approximately $818 USD per hectare. For comparison, a 2021 economic analysis for burley tobacco production in KY suggested that net returns after covering production costs would approximate $253 per hectare (Snell, 2021), which is dwarfed by the calculated economic impact of transplant RBQ ≤3.0.

Since assessment of transplant RBQ occurs early in the growing season, growers may use this in planning farm management activities, particularly labor. Most non-management tobacco production labor occurs through guest worker (such as H2A) programs, and early season recognition of reduced yields could save growers' labor costs up to 25% per worker, assuming the grower only utilizes the minimum guaranteed hours per guest worker (Roka and Guan, 2018). Though further replications are warranted, usage of the RBQ scale may not only be a way for growers to monitor PRR in their transplant crops, but in some cases, may improve growers' planning for field management and harvest labor needs.

5. Conclusion

The greenhouse floatbed fungicide treatments mefenoxam and etridiazole improve tobacco RBQ, as influenced by *P. myriotylum* inoculation. Higher average RBQ improves tobacco establishment and survival, and increases cured yield, though other production factors are also likely to influence these output variables. Application of the RBQ scale to tobacco transplants early in the season may help growers project yield estimates at the conclusion of curing tobacco crops.

Funding sources

This research was supported by Japan Tobacco International, Altria, and Philip Morris International.

Credit authorship contribution statement

Bob Pearce: Conceptualization, Methodology, Investigation, Writing – review and editing. William B. Barlow: Methodology, Investigation, Writing – review and editing. Emily E. Pfeufer: Conceptualization, Methodology, Investigation, Analysis, Visualization, Writing – original draft.

Disclaimers

1. Mention of trade names or commercial products in this publication is solely for the purpose of providing specific information and does not imply recommendation or endorsement by the U.S. Department of Agriculture.
2. USDA is an equal opportunity provider and employer.

Declaration of competing interest

The authors declare that they have no known competing financial interests or personal relationships that could have appeared to influence the work reported in this paper.

Data availability

Data will be made available on request.

Acknowledgements

The 2016, 2017, and 2018 trials were foci of the following University of Kentucky Cooperative Extension interns' experiences, respectively: Fabian Leon, Grace Ragain, and Sarah Jo Diamond. The authors are grateful to the following for their technical assistance: Jack Zeleznik, Haylee Taylor, Ed Dixon, William Pearce, Erica Fealko, April Lamb, and Dr. Hua Li. The corresponding author appreciates statistical discussions and feedback from Dr. Bill Turechek, as well as general input from Lindsay Harrison on manuscript development. The authors also thank six reviewers for their thoughtful critiques.

Appendix A. Supplementary data

Supplementary data to this article can be found online at https://doi.org/10.1016/j.cropro.2022.106152.

References

Burley and Dark Tobacco Production Guide. 2021-2022. Editors: andy Bailey and Bob Pearce. University of Kentucky extension publication ID-160. http://www2.ca.uky.edu/agcomm/pubs/ID/ID160/ID160.pdf. (Accessed 7 July 2021).

Fortnum, B.A., Rideout, J., Martin, S.B., Gooden, D., 2000. Nutrient solution temperature affects Pythium root rot of tobacco in greenhouse float systems. Plant Dis. 84, 289–294. https://doi.org/10.1094/PDIS.2000.84.3.289.

Gutierrez, W., Melton, T., Mila, A., 2012. Pythium root rot of flue-cured tobacco seedlings produced in greenhouses: factors associated with its occurrence and chemical control. Plant Health Prog. https://doi.org/10.1094/PHP-2012-0925-01-RS.

Krasnow, C.S., Hausbeck, M.K., 2017. Influence of pH and etridiazole on *Pythium* species. Am. Soc. Hort. Sci. 27, 367–374. https://doi.org/10.21273/HORTTECH03633-16.

Lookabaugh, E.C., Ivors, K.L., Shew, B.B., 2015. Mefenoxam sensitivity, aggressiveness, and identification of *Pythium* species causing root rot on floriculture crops in North Carolina. Plant Dis. 99, 1550–1558. https://doi.org/10.1094/PDIS-02-15-0232-RE.

McGehee, C.S., Raudales, R.E., 2021. Pathogenicity and mefenoxam sensitivity of *Pythium, Globisporangium*, and *Fusarium* isolates from coconut coir and rockwool in marijuana (*Cannibis sativa* L.) production. Front. Agron. https://doi.org/10.3389/fagro.2021.706138.

Moorman, G.W., Kang, S., Geiser, D.M., Kim, S.H., 2002. Identification and characterization of *Pythium* species associated with greenhouse floral crops in Pennsylvania. Plant Dis. 86, 1227–1231. https://doi.org/10.1094/PDIS.2002.86.11.1227.

Mufunda, F., Muzhinji, N., Sigobodhla, T., Marunda, M., Chinheya, C.C., Dimbi, S., 2017. Characterization of *Pythium* spp. associated with root rot of tobacco seedlings produced using the float tray system in Zimbabwe. J. Phytopathol. 165, 737–745. https://doi.org/10.1111/jph.12613.

Oxidate. Oxidate 2.0 product label. http://www.cdms.net/ldat/ldBKA000.pdf. (Accessed 9 August 2021).

Rey, P., Nodet, P., Tirilly, Y., 1997. *Pythium* F induce a minor but ubiquitous disease in tomato soilless cultures. J. Plant Pathol. 79, 173–180.

Robideau, G.P., de Cock, A.W.A.M., Coffey, M.D., Voglmayr, H., Brouwer, H., Bala, K., Chitty, D.W., DeSaulniers, N., Eggertson, Q.A., Gachon, C.M.M., Hu, C.-H., Kupper, F.C., Rintoul, T.A., Sarhan, E., Verstappen, E.C.P., Zhang, Y., Bonants, P.J.M., Ristaino, J.B., Levesque, C.A., 2011. DNA barcoding of oomycetes with cytochrome c oxidase subunit I and internal transcribed spacer. Mol. Ecol. Resources 11, 1002–1011. https://doi.org/10.1111/j.1755-0998.2011.03041.x.

Roka, F.M., Guan, Z., 2018. Farm labor management treds in Florida, USA – challenges and opportunities. Int. J. Agricultural Manag. 7 (1), 79–87. https://doi.org/10.22004/ag.econ.292479.

Schwarz, D., Beuch, U., Bandte, M., Fakhro, C., Buttner, C., Obermeier, C., 2010. Spread and interaction of Pepino mosaic virus (PepMV) and *Pythium aphanidermatum* in a closed nutrient solution recirculation system: effects on tomato growth and yield. Plant Pathol. (Lond.) 59, 443–452. https://doi.org/10.1111/j.1365-3059.2009.02229.x.

Sigobodhla, T.E., Dimbi, S., Masuka, A.J., 2010. First report of *Pythium myriotylum* causing root and stem rot on tobacco in Zimbabwe. Plant Dis. 94 (8), 1067. https://doi.org/10.1094/PDIS-94-8-1067C.

Snell, W., 2021. 2021 tobacco budgets. Economic and policy update. University of Kentucky Agricultural Economics 21 (2). https://agecon.ca.uky.edu/files/2021_tobacco_budgets.pdf. (Accessed 9 February 2022).

Stanghellini, M., Kronland, W.C., 1986. Yield loss in hydroponically grown lettuce attributed to subclinical infection of feeder roots by *Pythium dissotocum*. Plant Dis. 70, 1053–1056. https://doi.org/10.1094/PD-70-1053.

Terramaster. Terramaster 4EC product label. http://www.cdms.net/ldat/ld5GJ004.pdf. (Accessed 9 August 2021).

United States Department of Agriculture, National Agricultural Statistics Service Quickstats, 2022. Searched Prices Received for Burley Tobacco in Kentucky, pp. 1990–2020. https://www.nass.usda.gov/Quick_Stats/Lite/result.php?81B31409-6988-3ABD-9239-C4B08DFDE529. (Accessed 8 February 2022).

Zhang, X., 2021. Ecology and Management of *Pythium* Species in Float Greenhouse Tobacco Transplant Production. Virginia Tech. PhD Dissertation. http://hdl.handle.net/10919/101779.

Zhang, X., Johnson, C.S., Reed, D., 2021. Management of *Pythium myriotylum* in tobacco transplant production greenhouses. Plant Health Prog. https://doi.org/10.1094/PHP-03-21-0062-FI.

Plant Stress 9 (2023) 100194

Contents lists available at ScienceDirect

Plant Stress

journal homepage: www.sciencedirect.com/journal/plant-stress

Differential oxidative stress homeostasis in two burley tobacco varieties is linked to different peroxisomal glycolate oxidase levels

Jasmina Kurepa , Jan A. Smalle *

Department of Plant and Soil Sciences, Plant Physiology, Biochemistry, Molecular Biology Program, University of Kentucky, Lexington, KY 40546, USA

ARTICLE INFO

Keywords:
Oxidative stress
Tobacco
Untargeted metabolomics
Glycolate oxidase
Peroxisomes

ABSTRACT

Previous analyses of burley tobacco varieties KT 204LC and NCBH 129LC revealed that NCBH 129LC has a higher oxidative stress tolerance level and accumulates more hydrogen peroxide. We conducted untargeted metabolomics analyses to deepen our understanding of these varietal differences in redox status, and here, we show that KT 204LC and NCBH 129LC significantly differ in lipid metabolism, with NCBH 129LC containing more lipids than KT 204LC. Considering that NCBH 129LC also has more hydrogen peroxide and that peroxisomes play a major role in hydrogen peroxide production and lipid metabolism, we next analyzed peroxisomal markers. Glycolate oxidase, the key photorespiratory enzyme and a significant producer of hydrogen peroxide, accumulated significantly higher in NCBH 129LC. Our data suggest that differences in the oxidative stress status of burley varieties KT 204LC and NCBH 129LC are – at least partially - caused by different peroxisomal activities of the two varieties.

1. Introduction

The concept of the 'Oxygen Paradox' emphasizes the critical role of oxygen in the survival of aerobic organisms while also recognizing the inherent risks it presents to their existence (Davies, 1995; Halliwell, 2006). This paradox holds particular relevance for photosynthetic organisms. To survive in an oxygen-rich environment while generating oxygen, plants have an array of antioxidant compounds and antioxidant enzymes that inactivate reactive oxygen species (ROS) (Agati et al., 2012; Dixon and Paiva, 1995; Grene, 2002; Hasanuzzaman et al., 2017; Mittler et al., 2004; Noctor and Foyer, 1998; Sies, 2015). ROS are a natural byproduct of cellular metabolism, and under optimal conditions, antioxidant defense systems can neutralize the excess ROS and the cell can either repair any oxidative damage or remove the damaged constituents (Halliwell, 2006). However, many extrinsic and intrinsic conditions can disbalance the rate of ROS production and the capacity for antioxidant defense and repair, which is - by definition - oxidative stress Given that oxidative stress poses a universal challenge to aerobic organisms, comprehensive analyses have been undertaken to investigate responses to oxidative stress from multiple perspectives. For instance, researchers have employed targeted and untargeted metabolomic analyses to assess the effects of oxidative stress across various organisms, from bacteria to plants. These investigations aimed to elucidate the wide-ranging metabolic consequences of oxidative stress and establish oxidative stress biomarkers (Doran et al., 2017; Noctor et al., 2015; Pan et al., 2021). The metabolomic response to oxidative stress was shown to engage multiple metabolic pathways whose identity may differ dependent on the nature of the oxidative stress inducer (Doran et al., 2017). Despite that, some responses are common to all organisms and all types of oxidative stress (Doran et al., 2017; Noctor et al., 2015; Pan et al., 2021). For example, glutathione, which plays a critical role in the antioxidant defense in eukaryotes, gram-negative and some gram-positive bacteria, is viewed as a universal marker for changes in cellular redox state (Noctor et al., 2015; Pan et al., 2021). The complexity of metabolic responses to oxidative stress is further increased by genetic diversity within each species, as very different metabolomes and different responses to stress can characterize different genotypes (Villate et al., 2021).

Previously, we analyzed the oxidative stress status of two burley tobacco cultivars, KT 204LC and NCBH 129LC, which differ in their capacity to accumulate tobacco-specific nitrosamines (TSNAs), carcinogenic compounds whose reduction in tobacco products has become a commercial priority for the tobacco industry, and whose formation is potentially linked to the oxidative stress status of tobacco cells (Kurepa et al., 2021). Our findings demonstrated that NCBH 129LC contains higher levels of ROS hydrogen peroxide (H_2O_2) compared to KT 204LC (Kurepa et al., 2021). H_2O_2 has the potential to cause cellular damage by

* Corresponding author.
E-mail address: jsmalle@uky.edu (J.A. Smalle).

https://doi.org/10.1016/j.stress.2023.100194
Received 7 June 2023; Received in revised form 12 July 2023; Accepted 1 August 2023
Available online 2 August 2023

Abbreviations

ROS	reactive oxygen species
H_2O_2	hydrogen peroxide
PQ	paraquat
GSSG	glutathione disulfide
CSSG	cysteine glutathione disulfide
HODE	hydroxyoctadecadienoic acid
PCA	principal component analysis
OPLS-DA	orthogonal signal correction partial least squares discriminant analysis
MSEA	metabolite set enrichment analysis
MGDG	monogalactosyldiacylglycerol
DGDG	digalactosyldiacylglycerol
SQDG	sulfoquinovosyldiacylglycerol
Pex14p	Peroxine 14
HPR	hydroxypyruvate reductase
GLO	glycolate oxidase
CAT	catalase
CoA	Coenzyme A
TSNAs	tobacco-specific nitrosamines

directly oxidizing specific amino acids such as cysteine, methionine, and histidine within proteins (Davies, 2016). Furthermore, H_2O_2 can participate in reactions that generate other highly reactive oxygen species, including hydroxyl radicals, which can further contribute to oxidative damage (Davies, 2016). Consistent with these observations, our previous study revealed that NCBH 129LC extracts contained a greater abundance of oxidatively damaged proteins compared to KT 204LC (Kurepa et al., 2021). Aside from its role as a damaging oxidative stress agent, H_2O_2 also serves as a signaling molecule and is involved in cellular adaptation to stress conditions by activating protective mechanisms (Smirnoff and Arnaud, 2019). Hence, it is not surprising that under normal growth conditions, NCBH 129LC exhibits heightened engagement of oxidative stress defense mechanisms, leading to enhanced tolerance against the deleterious effects of the superoxide radical-generating redox-active herbicide paraquat (PQ) (Kurepa et al., 2021; Bus and Gibson, 1984). Here, using a metabolomics-driven strategy, we have investigated the underlying cause for the differences in oxidative stress homeostasis between these burley varieties. We find that KT204 LC and NCBH 129LC metabolomes differ substantially under normal growth conditions, that PQ-induced oxidative stress differentially affects the metabolomes, and that NCBH 129LC contains more of the H_2O_2-generating enzyme glycolate oxidase.

2. Materials and methods

2.1. Plant growth and treatment conditions

KT 204LC and NCBH 129LC seeds (obtained from F.W. Rickard Seds, Winchester, KY) were surface sterilized (5 min in 70% ethanol, followed by 20 min in 50% commercial bleach solution and three rinses in sterile water) and sown in vessels for plant tissue culture (Sigma-Aldrich) containing 100 ml Murashige and Skoog medium (pH 5.7; MS, Phytotechnology) with 3% sucrose and 0.8% phytoagar (Phytotechnology). Seedlings were grown in a controlled environment chamber under continuous light (25 °C; 80 μmol m^{-2} s^{-1}) for two months. Laminas of three third and three fourth leaves of the two-month-old plants (each leaf pair from a different growth vessel) were pooled and incubated in either water (control) or 100 μM PQ (aqueous solution of methyl viologen, Sigma-Aldrich) for 4 h at 25 °C in light (80 μmol m^{-2} s^{-1}). The tissue was blotted dry, snap-frozen, and stored at −80 °C for further analyses.

2.2. Metabolomics analyses

Frozen leaf tissue was mixed with 5 vol of HPLC-grade ethanol and disrupted with zirconium beads using the BeadBug™ Microtube Homogenizer (4000 rpm for 5 min at room temperature). Samples were centrifuged, and the supernatants were sent for untargeted metabolomic analysis to the Proteomics & Mass Spectrometry Facility at the Danforth Plant Science Center. The LC-MS/MS platform used was Q-Exactive with 50,000 mass resolution (Thermo-Fisher Scientific) with TriVersa Nanomate (Advion) and 2DLC Ultra NanoLC (Eksigent). The samples were injected into a 0.5 × 50 mm Supleco Bioshell C4 column using 0.1% formic acid in water (A) and acetonitrile (B). The gradient was as follows: 25%B for 3 min followed by a linear ramp to 100%B over 11 min, a hold at 100%B for 5 min, then a ramp back to 25%B over one min followed by re-equilibration for 10 min. Data were collected in polarity switching mode, MS/MS spectra were acquired in a top 5 data-dependent acquisition experiment. Data were preprocessed and viewed using the Elements software package (www.proteomesoftware.com). Peak assignments were made based on exact mass, isotope pattern match, and MS/MS spectral match against the NIST spectral database.

Preprocessed datasets, limited to metabolites fulfilling identification criteria (ID score ≥75), were exported from Elements as peak intensity tables (*.csv) and analyzed using MetaboAnalyst 3.0 (www.metaboanalyst.ca (Xia et al., 2009)). After missing value imputations and data filtering, data were normalized by sum, log-transformed (base 10), and autoscaled. Statistical analyses, Biomarker Analyses, and Metabolic Pathway Enrichment Analysis were done using Statistical Module, Biomarker, and Pathway Analyses Modules in MetaboAnalyst. Alternatively, the normalized preprocessed data were analyzed using the R package *mseapca* (Yamamoto et al., 2014). Data were scaled to zero mean, and PC scores, factor loadings, and *p*- and *q*-value (Benjamini and Hochberg) were calculated. Metabolites with significant factor loadings were sorted into chemical classes or subclasses following the Human Metabolomic Database (HMDB, http://www.hmdb.ca/) classification. Hierarchical clustering analysis was done using the R package *ComplexHeatmap* (Gu et al., 2016) using Manhattan clustering distance and ward.D2 clustering method. Venn Diagram analyses were done using the *VennDiagram* package (Chen and Boutros, 2011).

2.3. Immunoblotting

Protein extraction and immunoblotting analyses were performed as previously described (Kurepa et al., 2021). Protein extractions were done on pools of laminas of three third and three fourth leaves of the two-month-old plants. Immunoblotting experiments were done with five biological replicates. Primary antibodies used were anti-Peroxine 14 (anti-Pex14p; dilution 1:5000; Agrisera AS08 372), anti-hydroxypyruvate reductase (anti-HPR; 1:5000; Agrisera AS11 1797), anti-glycolate oxidase (anti-GLO; 1:1000; Agrisera AS14 2772), and anti-catalase (anti-CAT; 1:1000; Agrisera AS09 501). The secondary antibodies used (horseradish peroxidase-conjugated goat anti-rabbit IgG antibodies) were obtained from BioRad. Immunoblots were developed using SuperSignal West Femto substrate (Thermo-Pierce) using a ChemiDoc™ XRS molecular imager (Bio-Rad). The signal intensities were measured using QuantityOne software (Bio-Rad). Statistical analyses of the signal intensities were done using GraphPad Prism 9. Statistical comparison of means within groups was performed using one-way analysis of variance (ANOVA), followed by Tukey's multiple comparisons test. P-values ≥0.05 were considered non-significant.

3. Results and discussion

3.1. Analyses of oxidative stress markers

We performed untargeted metabolomic analyses to profile the

metabolic changes in KT 204LC and NCBH 129LC leaves treated with PQ for 4 h at room temperature under continuous light. Before detailed analyses of the metabolomic dataset, we analyzed the abundance of a selection of oxidative stress markers to validate the treatment. Our previous analyses showed that leaves of soilgrown NCBH 129LC contained more glutathione than KT 204LC (Kurepa et al., 2021). For untargeted metabolomic analyses, we used axenically grown plants (Fig. 1A), and to test whether glutathione levels differ between varieties independently of growth conditions and to validate the PQ treatment, we extracted the data pertinent to glutathione from the metabolomic dataset (Fig. 1B). Whereas reduced glutathione (GSH) was not detected in our dataset, glutathione disulfide (GSSG) and cysteine glutathione disulfide (CSSG), which are both formed upon oxidative stress (Noctor et al., 2012), were detected and were more abundant in the untreated NCBH 129LC than in untreated KT 204LC leaf extracts (Fig. 1B). Following PQ treatment, the levels of GSSG and CSSG increased in KT 204LC but not in NCBH 129LC (Fig. 1B). Since glutathione is widely recognized as a crucial component of the antioxidant defense system in eukaryotes and is considered a universal marker for cellular redox changes (Noctor et al., 2015), we can conclude that the redox state in NCBH 129LC remained unchanged in response to PQ treatment and that glutathione serves as a valid marker for PQ-induced oxidative stress in KT 204LC, but not in NCBH 129LC. As previously reported, NCBH 129LC consistently contains higher levels of glutathione and exhibits a higher tolerance to PQ-induced oxidative stress (Kurepa et al., 2021). This is here illustrated by the absence of any increase in the oxidized forms of glutathione (GSSG and CSSG) in response to PQ treatment in NCBH 129LC.

Next, we analyzed the abundance of an oxidative stress marker that points to oxidative stress damage rather than to oxidative stress defense levels (as is the case for glutathione). Because oxidative degradation of lipids is one of the major results of oxidative stress-induced damage, stable oxidation products of linoleic acid (hydroxyoctadecadienoic acids (HODEs)) are often used as a biomarker of perceived oxidative stress

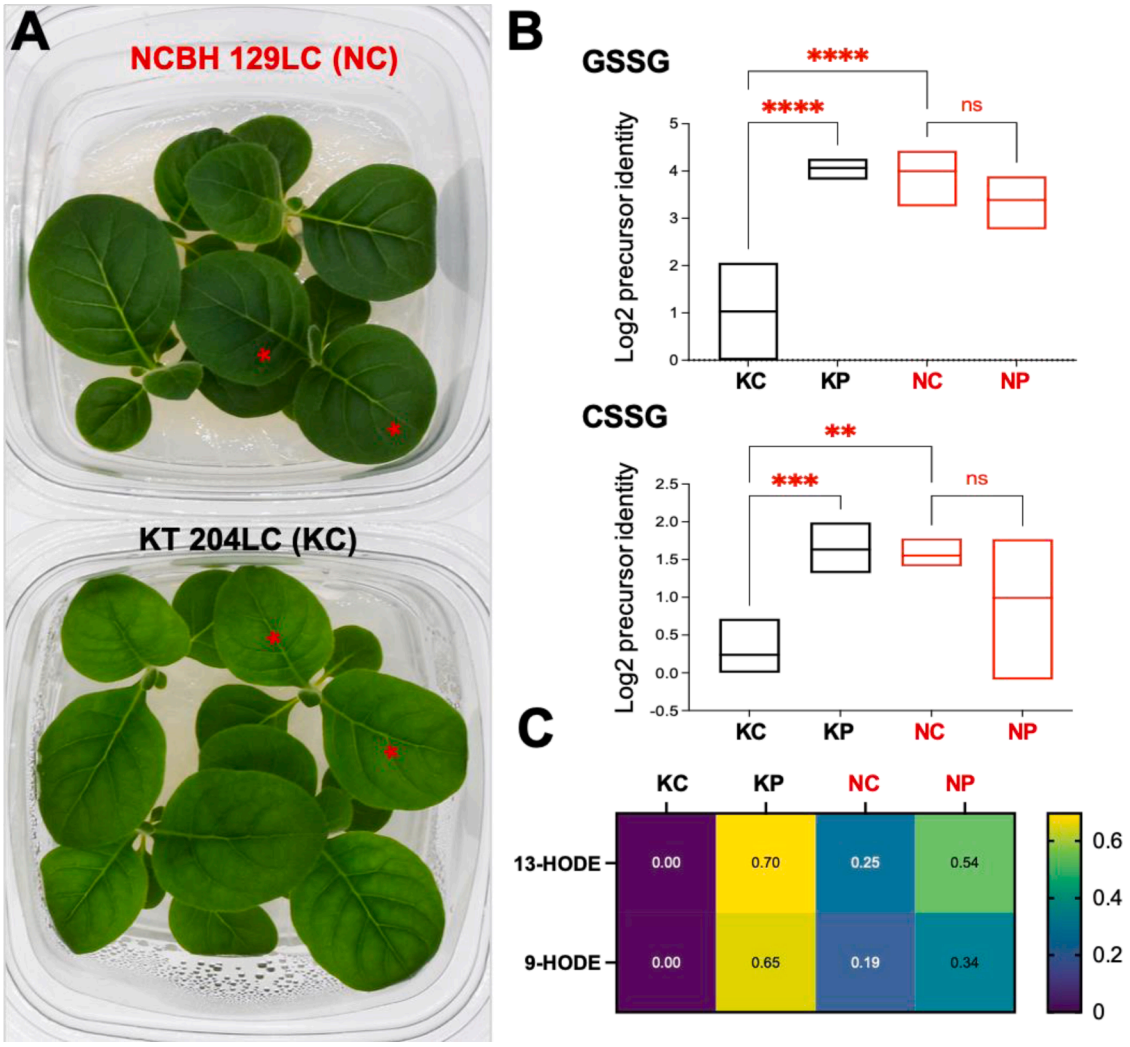

Fig. 1. Analyses of oxidative stress markers in KT 204LC and NCBH 129LC.

A. Representative plants used for metabolomic analyses. KT 204LC and NCBH 129LC seeds were sterilized and planted on Murashige and Skoog media with 3% sucrose and 0.8% agar. Plants were grown for four weeks in a controlled environment chamber before sampling. Red asterisk marks the developmental stage of the sampled leaves.

B. Average log2 precursor intensity of oxidized glutathione (GSSG) and cysteine glutathione disulfide (CSSG) in untreated KT 204LC and NCBH 129LC leaves (KC and NC, respectively) and paraquat-treated KT 204LC and NCBH 129LC leaves (KP and NP). Floating bars indicate the minimum and maximum intensity (top and bottom of the box) and mean (line within the box). Data were analyzed with one-way ANOVA ($P < 0.0001$ for GSSG and $P = 0.0003$ for CSSG, $n = 3$). Tukey's multiple comparison test was used to calculate the significance of the difference between samples (****, $P \leq 0.0001$; ***, $P \leq 0.001$; **, $P \leq 0.01$; ns, not significant).

C. Heatmap profile of 13-HODE (12-oxo,13-hydroxy-9Z-octadecenoic acid) and 9-HODE (2R-hydroxy-9Z,12Z-octadecadienoic acid) levels. Average ($n = 3$) log2 fold change compared to KC is shown.

(Yoshida and Niki, 2004; Yoshida et al., 2013). HODE levels were significantly higher in the untreated NCBH 129LC plants compared to KT 204LC plants ($p = 0.01$). After PQ treatment, HODE levels significantly increased in KT 204LC ($P < 0.0001$; ANOVA followed by Tukey's multiple comparison test) but remained virtually unchanged ($P = 0.0634$; ANOVA followed by Tukey's multiple comparison test) in NCBH 129LC (Fig. 1C). Together, these analyses validated the effectiveness of the PQ treatment and confirmed our previous finding that NCBH 129LC is more tolerant to oxidative stress treatment than KT 204LC (Kurepa et al., 2021).

3.2. Metabolic response to PQ is attenuated in NCBH 129LC

To reveal global metabolomic changes after PQ treatment, we used two multivariate methods, principal component analysis (PCA) and orthogonal signal correction partial least squares discriminant analysis (OPLS-DA) (Fig. 2). The PCA score plot shows a distinct separation of three groups (Fig. 2A). Two groups represent the separation of the KT 204LC control group from the NCBH 129LC control group, and the third group encompassed the PQ-treated samples of both varieties. Orthogonal arrangement of the KT 204LC metabolome ellipses before and after PQ treatment, as opposed to the parallel arrangement observed for NCBH 129LC metabolome ellipses, suggested that the global metabolic response to oxidative stress in NCBH 129LC was attenuated compared to those in KT 204LC. These results further validate our previous conclusion that the responses to oxidative stress differ between KT 204LC and NCBH 129LC. The OPLS-DA analysis, which maximizes the variance between groups in a single dimension, resulted in a scores plot displaying improved separation between the untreated and treated groups of both varieties (Fig. 2B). Therefore, we reached two conclusions. First, the metabolomes of untreated KT 204LC and NCBH 129LC are distinct, and second, NCBH 129LC and KT 204LC metabolic responses to oxidative stress are different.

3.3. Glycerophospholipid profile is the most significant difference between varieties

To uncover the unique metabolic fingerprints of each variety, we first analyzed the metabolomes of untreated KT 204LC and NCBH 129LC. The untreated samples were analyzed using three approaches. First, we performed metabolite set enrichment analysis (MSEA) for factor loading in PCA using the *mseapca* package (Yamamoto et al., 2014). PCA analyses of 2582 metabolites (ID score ≥ 0.75) revealed an outlier sample (NCBH 129LC #1, NC1), which was excluded from further MSEA computations (Fig. 3A). The statistical hypothesis testing for factor loading in PC1 revealed 153 candidate endo-metabolites as varietal markers (Supplemental Table S1). The most striking difference between varieties was in the level of lipids and lipid-like molecules (Fig. 3B): 55% of significant metabolites ($P < 0.01$) were lipids, 27% were organic acids and derivatives, and 13% were phenylpropanoids and polyketides (Supplemental Table S1). Hierarchical clustering analyses of lipids with statistically significant factor loading in PC1 showed an overabundance of lipids in the NCBH 129LC variety (Fig. 3C).

In the second approach, we performed Pathway Analyses of significant metabolites using the MetaboAnalyst Pathway Analyses Module (Xia et al., 2009). Analyses (done against Arabidopsis Kegg pathways using the Fishers' exact test) showed that the most significantly different divergent pathway ($P = 0.030496$) between varieties was glycerophospholipid metabolism followed by the linoleic acid metabolic pathway ($P = 0.073483$) (Fig. 3D).

Third, we analyzed metabolites that significantly differed between untreated KT 204LC and NCBH 129LC (*t*-test with the Benjamini-Hochberg procedure; $q = 0.05$) using the MetaboAnalyst Biomarker Analyses Module. Classical univariate ROC curve analyses showed that of the 30 most significant biomarkers, 77% were lipids, and 61% of lipid biomarkers were glycerophospholipids (Supplemental Table S2). Since glycerophospholipids are major constituents of cellular membranes, this suggests that many processes that depend on membrane fluidity and integrity may also differ between varieties.

Interestingly, two of the top 30 biomarkers were thylakoid glycoglycerolipids (Supplemental Table S2). Compared to the other cellular compartments, chloroplasts are characterized by a very low phosphoglycerolipids content and a very high content of glycoglycerolipids such as monogalactosyldiacylglycerol (MGDG), digalactosyldiacylglycerol (DGDG) and sulfoquinovosyldiacylglycerol (SQDG) (Boudière et al., 2014). Analyses of the abundance of identified (ID ≥ 0.75) glycoglycerolipids showed that all were more abundant in NCBH 129LC (Student's *t*-test, $P \leq 0.001$; Fig. 3D). Given the essential role of

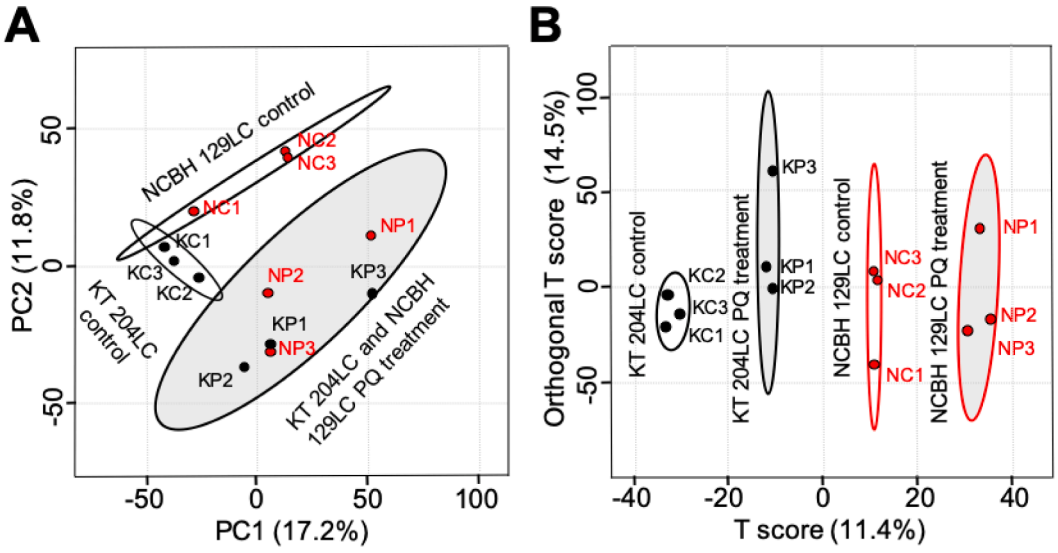

Fig. 2. Multivariate analyses of metabolomes of control and paraquat-treated burley varieties.
The principle component analysis (A) and orthogonal partial least-squares discriminant analysis (B) score plots of NCBH 129LC (N) and KT 204LC (K) leaves treated with water (C, control) or 100 μM PQ (P) for 4 h in the light at room temperature. The models were calculated using LC-MS/MS metabolomics data from three replicates per treatment, with each replicate containing a pool of laminar tissues of separate plants. Each point represents a sample, and the distance between points reflects the degree of metabolic distinction.

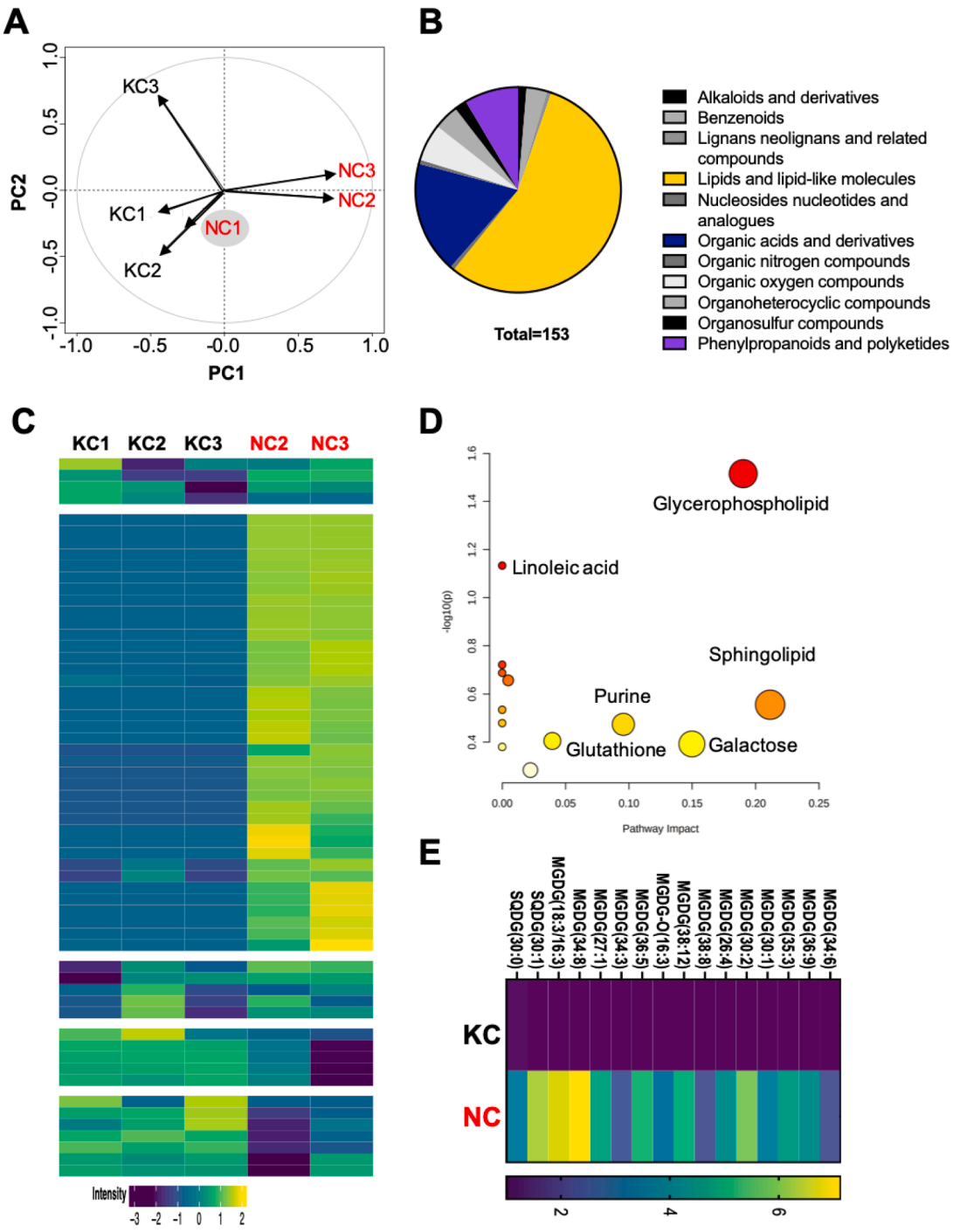

Fig. 3. Analyses of the significantly different metabolites between lines

A. The principle component analysis score plot of control NCBH 129LC (NC) and KT 204LC (KC) shows a separation of metabolomes by variety. The outlier sample (NBCH 129LC, NC1; shaded) was excluded from further analyses.

B. Metabolite classification analysis. Pie chart of the classes of metabolites identified as significantly different between varieties. Classification is based on chemical superclass as defined by HMDB.

C. Heatmap showing the abundance of lipids with statistically significant factor loading in PC1 ($p < 0.01$) in burley varieties NCBH 129LC and KT 204LC. Hierarchical clustering analysis was performed using the Manhattan correlation as the distance measure. The color intensity scale is positioned below the heatmap. KC, KT 204LC control extract; NC, NCBH 129LC control extract.

D. Metabolic Pathways identified as enriched among the metabolites that significantly differed in abundance between KT 204LC and NCBH 109LC. Pathway Impact Score in the x-axis represents the impact of the enriched pathways and "–logP" in the y-axis refers to the negative natural logarithmic value of the original P value from statistical analysis of pathway difference between varieties. The size of each bullet represents the impact value, and the color of each bullet represents the significance of the enrichment. The most significant pathways are marked.

E. Heatmap analyses of thylakoid glycoglycerolipids. Average normalized log10 precursor intensity of molecules that were significantly different between varieties (Student's *t*-test compared to untreated KT 204LC (KC)) is presented. MGDG, monogalactosyldiacylglycerol; SQDG, sulfoquinovosyldiacylglycerol.

glycoglycerolipids in the structural stabilization and functionality of photosystems (Boudière et al., 2014), this suggests that there could be potential variations in the photosynthetic capacities of these two varieties (at least, when cultivated in axenic cultures). In addition to its vital role in establishing and maintaining the structure and function of the chloroplast, thylakoid glycoglycerolipids, and MGDG in particular, have been demonstrated to be associated with stress tolerance (Omoto et al., 2016; Farmer and Mueller, 2013; Schmid-Siegert et al., 2016; Wang et al., 2014; Garab et al., 2000). For instance, overexpressing a rice MGDG synthase in tobacco has been shown to enhance tolerance to salt stress (Wang et al., 2014). Considering these findings, along with our results demonstrating the higher MGDG content in NCBH 129LC, we propose that the increased levels of MGDG may significantly contribute to the enhanced tolerance exhibited by NCBH 129LC.

3.4. PQ response biomarkers

The GSSG and HODE level analyses (Fig. 1B,C) and PCA (Fig. 2), together with the results of our previous study (Kurepa et al., 2021), suggested that the metabolomes of PQ-treated NCBH 129LC and PQ-treated KT 204LC largely overlap. However, it remained possible that there are essential differences between these two varieties in their responses to PQ. To investigate this, all highly significant metabolites (ID $\geq$ 0.9; Students *t*-test with false-discovery rate controlled with Benjamin-Hockberg procedure, q-value of 0.05) were sorted into two subsets (untreated KT 204LC vs. treated KT 204LC and untreated NCBH 129LC vs. treated NCBH 129LC) and analyzed using the MetaboAnalyst Biomarker Module. These analyses identified 22 KT 204LC-specific and 14 NCBH 129LC-specific PQ biomarkers (Supplemental Table S3), ten of which were common to both sets (Fig. 4A). One of the common markers was flavin mononucleotide (FMN), an essential cofactor for many oxidoreductases, which are known to mitigate oxidative stress (Chen et al., 2020; Sinha et al., 2020). FMN levels followed the pattern observed for oxidized glutathione species and HODE: FMN levels were higher in the untreated NCBH 129LC than in untreated KT 204LC, and PQ treatment led to an increase in KT 204LC but not in NCBH 129LC (Fig. 4B). NCBH 129LC-specific PQ biomarkers included two basic metabolites: nicotinamide adenine dinucleotide (NAD) and glucose-6-phosphate (G6P) (Fig. 4C). NAD is another coenzyme involved in a myriad of metabolic processes. Its reduced form plays an essential role in regulating the redox state of the cell in all eukaryotes by linking H_2O_2 reduction to the glutathione pool in the Foyer-Halliwell-Asada cycle (Noctor et al., 2015, 2012; Hashida et al., 2009; Massudi et al., 2012). NAD levels were higher in untreated NCBH 129LC compared to KT 204LC, but – in contrast to FMN – PQ treatment led to an increase in NAD levels in both varieties (Fig. 4C). This result agrees with the well-established role of NAD in alleviating oxidative stress on the one hand (Noctor et al., 2015, 2012; Hashida et al., 2009; Massudi et al., 2012) and on the other, our findings that the steady-state level of oxidative stress is higher in untreated NCBH 129LC (Kurepa et al., 2021). G6P is the starting molecule of the oxidative pentose phosphate pathway, which is one of the major sources of another principal reducing molecule, nicotinamide adenine dinucleotide phosphate (NADPH). G6P dehydrogenase, the first and rate-limiting enzyme of the pentose phosphate pathway, was long

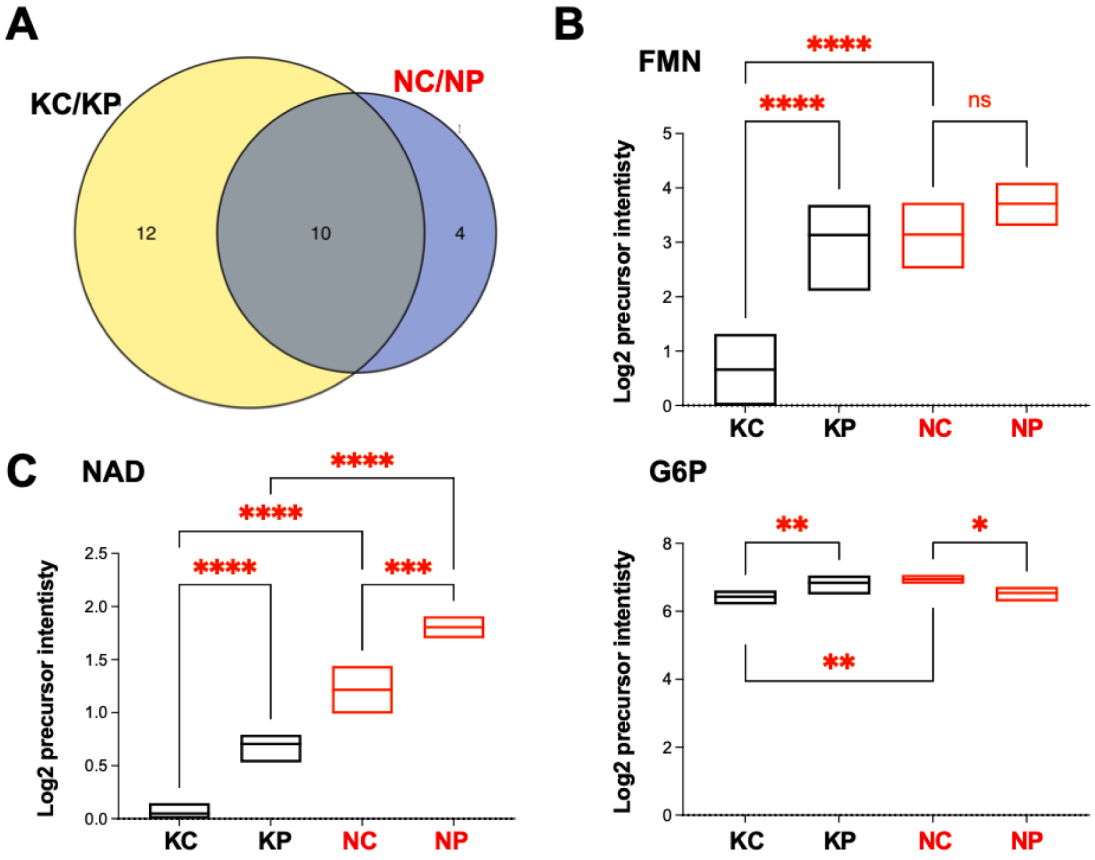

Fig. 4. Paraquat biomarkers in tobacco varieties KT 204LC and NCBH 129LC.
A. Venn diagram showing the number of shared and unique stress biomarkers of paraquat treatment in KT 204LC (KC/KP) and NCBH 129LC (NC/NP).
B. and C. Log2 precursor intensity of the shared biomarker flavine mononucleotide (FMN) and two of the NCBH 129 LC-specific markers, nicotinamide adenine dinucleotide (NAD) and glucose-6-phosphate (G6P). Floating bars indicate the minimum and maximum intensity and mean. Data were analyzed with one-way ANOVA ($P < 0.0001$ for GSSG and $P = 0.0003$ for CSSG, $n = 3$). Tukey's multiple comparison test was used to calculate the significance of the difference between samples (****, $P \leq 0.0001$; ***, $P \leq 0.001$; **, $P \leq 0.01$; ns, not significant).

recognized as an important antioxidant enzyme in eukaryotes (Efferth et al., 2006; Esposito, 2016). Metabolomic analyses of the catalase-deficient Arabidopsis *cat2* mutant revealed an increase in G6P levels (Noctor et al., 2015) and linked increased H_2O_2 levels with an increase in G6P. In line with those findings, G6P levels in NCBH 129LC were higher than in KT 204LC (Fig. 4C). PQ treatment led to an increase in G6P in KT 204LC and a small but significant decrease in NCBH 129LC (Fig. 4C). Thus, all three selected biomarkers are primary metabolites involved in redox regulation, and since all three were more abundant in untreated NCBH 129LC, they offer another example of this line's constitutively elevated oxidative stress defense.

3.5. Peroxisomal enzymes GLO and CAT are upregulated in NCBH 129LC

Untargeted metabolomic analyses, together with the results of our previous study (Kurepa et al., 2021), show that the NCHB 129LC variety has increased H_2O_2 levels, increased levels of several redox compounds, and higher levels of lipids (in particular, glycerophospholipids and glycoglycerolipids) compared to KT 204LC. Peroxisomes are known to be the major site of intracellular H_2O_2 production as well as the major cellular compartment in which H_2O_2 is detoxified (Corpas et al., 2020; Del Río, 2020; Foyer et al., 2009; Pan et al., 2020; Palma et al., 2020; Mhamdi et al., 2010). In addition to playing an essential role in H_2O_2 metabolism, plant peroxisomes are the only site of fatty acid oxidation and house several anabolic processes, including the synthesis of some glycerophospholipids (Corpas et al., 2020; Del Río, 2020; Foyer et al., 2009; Pan et al., 2020; Corpas and Barroso, 2017; Corpas et al., 2017, 2019; Mano and Nishimura, 2005; Wanders et al., 2010; Lodhi and Semenkovich, 2014). Based on these facts, we reasoned that peroxisomal activity might differ between the varieties.

To test this hypothesis, we analyzed the abundance of peroxisomal marker proteins in mature leaves (Fig. 5). All peroxisomal proteins are synthesized on free ribosomes in the cytosol and imported into peroxisomes (Walter and Erdmann, 2019). Peroxine 14 (Pex14p) binds with other peroxins and forms a docking protein complex that controls the import of proteins with a peroxisome targeting signal (Walter and Erdmann, 2019; Hayashi, 2000). Immunoblotting analyses showed that Pex14p levels were not significantly different between the samples (Fig. 5A,B). Analyses of Pex14p in mammalian cell lines showed that Pex14p is phosphorylated in response to oxidative stress (Okumoto et al., 2020). PQ treatment of tobacco leaves also led to the modification of Pex14p, as evidenced by the presence of higher-molecular weight versions of Pex14p in PQ-treated samples (Fig. 5A). Similar to other responses to oxidative stress that are attenuated in NCBH 129LC compared to KT 204LC, the level of modified Pex14p was significantly lower in PQ-treated NCBH 129LC (signal intensities of NCBH 129LC/KT 204LC $\simeq$ 0.6).

Next, we tested the abundance of three peroxisomal matrix proteins in the two varieties (Fig. 5A,B). Hydroxypyruvate reductase (HPR; EC 1.1.1.81) is used as a peroxisomal matrix marker and is involved in glycine, serine, and threonine metabolism (Kleczkowski and Edwards, 1989; Li et al., 2019), The only statistically significant difference in HPR levels observed was the decrease of HPR in NCBH 129LC after PQ treatment ($P = 0.026$, $n = 5$).

The second matrix protein tested was glycolate oxidase (GLO; EC 1.1.3.1), an enzyme essential for photorespiration that oxidizes glycolate to H_2O_2 and glyoxylate and is responsible for the generation of most of the peroxisomal H_2O_2 (Foyer et al., 2009; Esser et al., 2014; Rojas et al., 2012; Dellero et al., 2016). Immunoblotting analyses showed that GLO levels were higher in untreated NCBH 129LC than in untreated KT 204LC leaves ($P = 0.005$, $n = 5$). Arabidopsis plants overexpressing GLO in chloroplasts and rice plants overexpressing GLO have been analyzed previously (Fahnenstich et al., 2008, 2008; Cui et al., 2016). Low-level peroxisomal overexpression of GLO in rice resulted in growth stimulation of transgenic plants but no improvement in photosynthesis under normal grown conditions (Cui et al., 2016). However, overexpression plants performed better than the control under heat shock and high light, suggesting that the stress defense was strengthened by increasing photorespiration (Cui et al., 2016). Interestingly, rice plants overexpressing GLO were resistant to PQ, which is also one of the described stress phenotypes of NCBH 129LC plants (Kurepa et al., 2021; Cui et al., 2016). In addition, *glo* rice knockout mutants exhibited a reduction in H_2O_2 levels, accompanied by an increase in auxin IAA levels attributable to enhanced IAA synthesis (Li et al., 2021). This observation further confirms GLO as a main contributor to H_2O_2 production in plants. Moreover, as auxins are recognized for their significant involvement in stress tolerance regulation (Salvi et al., 2021; Kurepa and Smalle, 2022), this discovery further underscores the connection between GLO and stress defense mechanisms. PQ treatment increased GLO levels in both varieties, and the resulting GLO levels in treated NCBH 129LC and KT 204LC leaves did not significantly differ.

The third matrix protein tested was catalase (CAT; EC 1.11.1.6), the most important enzyme for peroxisomal detoxification of H_2O_2 (Corpas et al., 2020; Palma et al., 2020; Mhamdi et al., 2010). The CAT level was higher in the untreated NCBH 129LC plants than in KT 204LC, which is

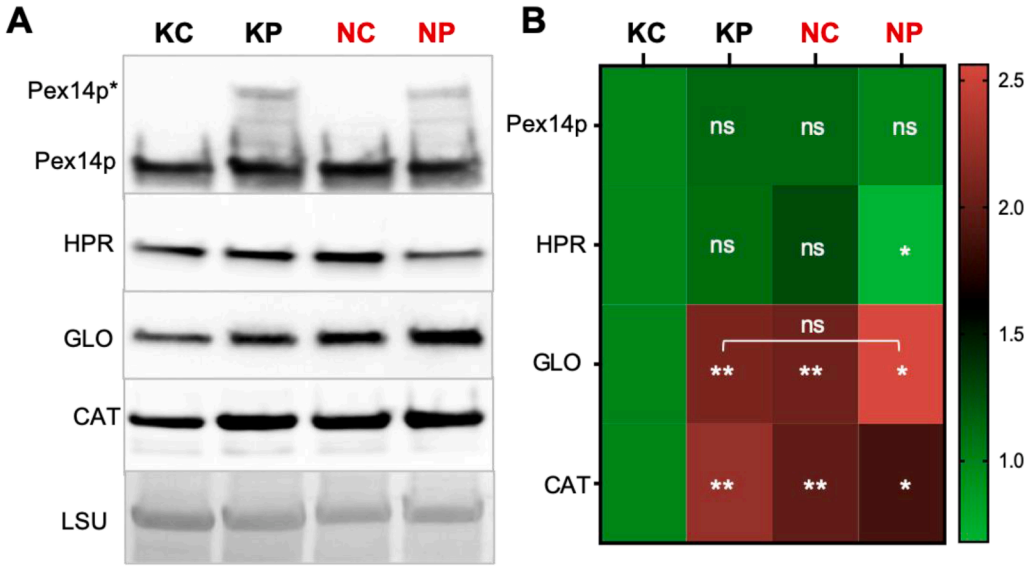

Fig. 5. Peroxisomal function differs between KT 204LC and NCBH 129LC.
A. Representative immunoblot images of peroxisomal marker proteins peroxine 14 (Pex14p), hydroxypyruvate reductase (HPR), glycolate oxidase (GLO), and catalase (CAT) in untreated and PQ-treated KT 204LC (KC and KP) and NCBH 129LC (NC and NP) leaves. Pex14*, stress-induced modified Pex14 isoform; LSU, large RuBisCO subunit (Ponceau S-stained membrane; loading control).
B. Heat map of normalized (KC=1) chemiluminescent immunoblotting signals. Data were analyzed with one-way ANOVA followed by Tukey's multiple comparison test (***, $P \leq 0.001$; **, $P \leq 0.01$; *, $P \leq 0.05$; ns, not significant; $n = 5$).

not surprising considering that NCBH 129LC tissues contain higher levels of H_2O_2 and that CAT gene expression is known to be induced in response to oxidative stress (Kurepa et al., 2021; Mhamdi et al., 2012). PQ-induced oxidative stress led to the upregulation of CAT levels in KT 204LC but not in NCBH 129LC, offering another example of the attenuated oxidative stress response in the latter variety.

4. Conclusions

We have previously shown that NCBH 129LC contains higher levels of H_2O_2 and the antioxidant GSH needed for H_2O_2 scavenging, combined with increased oxidative stress tolerance (Kurepa et al., 2021). In this study, we have identified several metabolome changes that can account for the difference in stress tolerance between the tested varieties. For example, we have observed variations in MGDG content as well as alterations in NAD, FMN, and G6P levels, which could all contribute to the distinct stress responses observed. However, to truly understand the primary cause underlying the differences in stress responses and to differentiate it from secondary changes in the metabolome (i.e., the adaptations of the metabolome in response to the alterations of the primary cause), targeted experimental analyses focused on investigating potential primary causes are essential. From this perspective, the elevated levels of the peroxisomal enzyme GLO in NCBH 129LC hold particular significance. GLO is responsible for the production of H_2O_2 as a by-product during glycolate oxidation, accounting for approximately 70% of total H_2O_2 production in C3 plants (Noctor et al., 2002). The increased GLO levels in NCBH 129LC are likely a contributing factor to the higher H_2O_2 content observed in this variety. Notably, previous studies have shown that overexpression of GLO can enhance stress tolerance (Cui et al., 2016). Therefore, the heightened levels of GLO, accompanied by increased levels of its essential co-factor FMN, may provide an explanation for the increased oxidative stress tolerance observed in NCBH 129LC, as the resulting increase in H_2O_2 is expected to serve as a signal triggering the oxidative stress defense system.

Another interesting difference between the NCBH 129LC and KT 204LC varieties is that they accumulate different levels of cancer-causing tobacco-specific nitrosamines (TSNAs) during the tobacco leaf curing process (Kurepa et al., 2021). Elevated oxidative stress has been previously implicated in increases in nitrosamine formation in animal species, including humans (Bartsch et al., 1989; Gutiérrez et al., 2014; Bartsch et al., 1988; Parnaud et al., 2000). Consequently, it would be of interest to investigate whether the heightened GLO activity and H_2O_2 production in NCBH 129LC are associated with increased TSNA accumulation in this variety. If a positive correlation is established, it opens up possibilities for potential interventions to mitigate TSNA accumulation during the curing process. For instance, partial suppression of GLO activity in aging tobacco leaves could be explored through approaches such as transgenic RNAi or the application of GLO inhibitors. Such interventions may potentially lead to the suppression of TSNA formation, thus providing a promising avenue for reducing the levels of these cancer-causing compounds during tobacco curing.

Funding sources

This work was supported by the Kentucky Tobacco Research and Development Center.

Appendix A. Supplementary data

Supplementary data to this article can be found online at …

Supplemental Table S1: List of metabolites that are significantly different between varieties

Supplemental Table S2: Varietal biomarkers

Supplemental Table S3: Paraquat treatment biomarkers

CRediT authorship contribution statement

Jasmina Kurepa: Conceptualization, Methodology, Investigation, Formal analysis, Writing – original draft. **Jan A. Smalle:** Conceptualization, Methodology, Supervision, Writing – review & editing, Resources.

Declaration of Competing Interest

The authors declare that they have no known competing financial interests or personal relationships that could have appeared to influence the work reported in this paper.

Data availability

Data will be made available on request.

Acknowledgments

We thank the Proteomics & Mass Spectrometry Facility at the Danforth Plant Science Center for performing the LC/MS/MS analyses.

Supplementary materials

Supplementary material associated with this article can be found, in the online version, at doi:10.1016/j.stress.2023.100194.

References

Agati, G., Azzarello, E., Pollastri, S., Tattini, M., 2012. Flavonoids as antioxidants in plants: location and functional significance. Plant Sci. 196, 67–76. https://doi.org/10.1016/j.plantsci.2012.07.014.

Bartsch, H., Ohshima, H., Pignatelli, B., 1988. Inhibitors of endogenous nitrosation. Mechanisms and implications in human cancer prevention. Mutat. Res. 202 (2), 307–324. https://doi.org/10.1016/0027-5107(88)90194-7.

Bartsch, H., Hietanen, E., Malaveille, C., 1989. Carcinogenic nitrosamines: free radical aspects of their action. Free Radic. Biol. Med. 7 (6), 637–644. https://doi.org/10.1016/0891-5849(89)90144-5.

Boudière, L., Michaud, M., Petroutsos, D., Rébeillé, F., Falconet, D., Bastien, O., Roy, S., Finazzi, G., Rolland, N., Jouhet, J., Block, M.A., Maréchal, E., 2014. Glycerolipids in photosynthesis: composition, synthesis and trafficking. Biochim. Biophys. Acta Bioenerg. 1837 (4), 470–480. https://doi.org/10.1016/j.bbabio.2013.09.007.

Bus, J.S., Gibson, J.E., 1984. Paraquat: model for oxidant-initiated toxicity. Environ. Health Perspect. 55, 37–46. https://doi.org/10.1289/ehp.845537.

Chen, H., Boutros, P.C, 2011. VennDiagram: a package for the generation of highly-customizable Venn and Euler diagrams in R. BMC Bioinform. 12 (1), 35. https://doi.org/10.1186/1471-2105-12-35.

Chen, X., Ji, B., Hao, X., Li, X., Eisele, F., Nyström, T., Petranovic, D, 2020. FMN reduces Amyloid-β toxicity in yeast by regulating redox status and cellular metabolism. Nat. Commun. 11 (1) https://doi.org/10.1038/s41467-020-14525-4.

Corpas, F.J., Barroso, J.B., 2017. Peroxisomal plant metabolism – an update on nitric oxide, Ca^{2+} and the NADPH recycling network. J. Cell Sci. 131 (2), jcs202978 https://doi.org/10.1242/jcs.202978.

Corpas, F.J., Barroso, J.B., Palma, J.M., Rodriguez-Ruiz, M., 2017. Plant peroxisomes: a nitro-oxidative cocktail. Redox. Biol. 11, 535–542. https://doi.org/10.1016/j.redox.2016.12.033.

Corpas, F.J., Del Rio, L.A., Palma, J.M., 2019. Plant peroxisomes at the crossroad of NO and H_2O_2 metabolism. J. Integr. Plant Biol. 61 (7), 803–816. https://doi.org/10.1111/jipb.12772.

Corpas, F.J., González-Gordo, S., Palma, J.M., 2020. Plant peroxisomes: a factory of reactive species. Front. Plant Sci. 11, 853. https://doi.org/10.3389/fpls.2020.00853.

Cui, L.L., Lu, Y.S., Li, Y., Yang, C., Peng, X.X, 2016. Overexpression of glycolate oxidase confers improved photosynthesis under high light and high temperature in rice. Front. Plant Sci. 7, 1165. https://doi.org/10.3389/fpls.2016.01165.

Davies, K.J., 1995. Oxidative stress: the paradox of aerobic life. Biochem. Soc. Symp. 61, 1–31. https://doi.org/10.1042/bss0610001.

Davies, M.J., 2016. Protein oxidation and peroxidation. Biochem. J. 473 (7), 805–825. https://doi.org/10.1042/bj20151227.

Del Río, L.A, 2020. Plant Peroxisomes and their Metabolism of ROS, RNS, and RSS. Springer International Publishing, Prog Bot, pp. 171–209.

Dellero, Y., Jossier, M., Schmitz, J., Maurino, V.G., Hodges, M., 2016. Photorespiratory glycolate–glyoxylate metabolism. J. Exp. Bot. 67 (10), 3041–3052. https://doi.org/10.1093/jxb/erw090.

Dixon, R.A., Paiva, N.L., 1995. Stress-Induced phenylpropanoid metabolism. Plant Cell 7 (7), 1085–1097. https://doi.org/10.1105/tpc.7.7.1085.

Doran, M.L., Knee, J.M., Wang, N., Rzezniczak, T.Z., Parkes, T.L., Li, L., Merritt, T.J.S., 2017. Metabolomic analysis of oxidative stress: superoxide dismutase mutation and paraquat induced stress in Drosophila melanogaster. Free Radic. Biol. Med. 113, 323–334. https://doi.org/10.1016/j.freeradbiomed.2017.10.011.

Efferth, T., Schwarzl, S.M., Smith, J., Osieka, R., 2006. Role of glucose-6-phosphate dehydrogenase for oxidative stress and apoptosis. Cell Death Differ. 13 (3), 527–528. https://doi.org/10.1038/sj.cdd.4401807.

Esposito, S., 2016. Nitrogen assimilation, abiotic stress and glucose 6-phosphate dehydrogenase: the full circle of reductants. Plants 5 (2). https://doi.org/10.3390/plants5020024 (Basel).

Esser, C., Kuhn, A., Groth, G., Lercher, M.J., Maurino, V.G., 2014. Plant and animal glycolate oxidases have a common eukaryotic ancestor and convergently duplicated to evolve long-chain 2-hydroxy acid oxidases. Mol. Biol. Evol. 31 (5), 1089–1101. https://doi.org/10.1093/molbev/msu041.

Fahnenstich, H., Flügge, U.I., Maurino, V.G., 2008a. *Arabidopsis thaliana* overexpressing glycolate oxidase in chloroplasts: h_2O_2-induced changes in primary metabolic pathways. Plant Signal. Behav. 3 (12), 1122–1125. https://doi.org/10.4161/psb.3.12.7040.

Fahnenstich, H., Scarpeci, T.E., Valle, E.M., Flügge, U.I., Maurino, V.G., 2008b. Generation of hydrogen peroxide in chloroplasts of Arabidopsis overexpressing glycolate oxidase as an inducible system to study oxidative stress. Plant Physiol. 148 (2), 719–729. https://doi.org/10.1104/pp.108.126789.

Farmer, E.E., Mueller, M.J., 2013. ROS-mediated lipid peroxidation and RES-activated signaling. Annu. Rev. Plant Biol. 64 (1), 429–450. https://doi.org/10.1146/annurev-arplant-050312-120132.

Foyer, C.H., Bloom, A.J., Queval, G., Noctor, G., 2009. Photorespiratory metabolism: genes, mutants, energetics, and redox signaling. Annu. Rev. Plant Biol. 60, 455–484. https://doi.org/10.1146/annurev.arplant.043008.091948.

Garab, G., Lohner, K., Laggner, P., Farkas, T., 2000. Self-regulation of the lipid content of membranes by non-bilayer lipids: a hypothesis. Trends Plant Sci. 5 (11), 489–494. https://doi.org/10.1016/s1360-1385(00)01767-2.

Grene R. (2002) Oxidative stress and acclimation mechanisms in plants. *The Arabidopsis Book:* 1, e0036-e0036. doi:10.1199/tab.0036.1.

Gu, Z., Eils, R., Schlesner, M., 2016. Complex heatmaps reveal patterns and correlations in multidimensional genomic data. Bioinformatics 32 (18), 2847–2849. https://doi.org/10.1093/bioinformatics/btw313.

Gutiérrez, A.J., Rubio, C., Caballero, J.M., Nitrites, Hardisson A., 2014. Encyclopedia of Toxicology. Wexler P, Ed., 3rd ed. Academic Press, Oxford, pp. 532–535.

Halliwell, B., 2006. Redox biology is a fundamental theme of aerobic life. Plant Physiol. 141 (2), 312–322. https://doi.org/10.1104/pp.106.077073.

Hasanuzzaman, M., Nahar, K., Anee, T.I., Fujita, M., 2017. Glutathione in plants: biosynthesis and physiological role in environmental stress tolerance. Physiol. Mol. Biol. Plants 23 (2), 249–268. https://doi.org/10.1007/s12298-017-0422-2.

Hashida, S.N., Takahashi, H., Uchimiya, H., 2009. The role of NAD biosynthesis in plant development and stress responses. Ann. Bot. 103 (6), 819–824. https://doi.org/10.1093/aob/mcp019.

Hayashi, M., 2000. AtPex14p maintains peroxisomal functions by determining protein targeting to three kinds of plant peroxisomes. EMBO J. 19 (21), 5701–5710. https://doi.org/10.1093/emboj/19.21.5701.

Kleczkowski, L.A., Edwards, G.E., 1989. Identification of hydroxypyruvate and glyoxylate reductases in maize leaves. Plant Physiol. 91 (1), 278–286. https://doi.org/10.1104/pp.91.1.278.

Kurepa, J., Smalle, J.A., 2022. Auxin/cytokinin antagonistic control of the shoot/root growth tatio and its relevance for adaptation to drought and nutrient deficiency stresses. Int. J. Mol. Sci. 23 (4), 1933. https://doi.org/10.3390/ijms23041933.

Kurepa, J., Shull, T.E., Fisher, A., Fisher, C., Ji, H., Smalle, J.A, 2021. Differential oxidative stress responses and tobacco-specific nitrosamine accumulation in two burley varieties. J. Plant Physiol. 261, 153429 https://doi.org/10.1016/j.jplph.2021.153429.

Li, J., Weraduwage, S.M., Preiser, A.L., Tietz, S., Weise, S.E., Strand, D.D., Froehlich, J.E., Kramer, D.M., Hu, J., Sharkey, T.D., 2019. A cytosolic bypass and G6P shunt in plants lacking peroxisomal hydroxypyruvate reductase. Plant Physiol. 180 (2), 783–792. https://doi.org/10.1104/pp.19.00256.

Li, X., Liao, M., Huang, J., Xu, Z., Lin, Z., Ye, N., Zhang, Z., Peng, X., 2021. Glycolate oxidase-dependent H_2O_2 production regulates IAA biosynthesis in rice. BMC Plant Biol. 21 (1), 326. https://doi.org/10.1186/s12870-021-03112-4.

Lodhi, J Irfan, Semenkovich, F Clay, 2014. Peroxisomes: a nexus for lipid metabolism and cellular signaling. Cell Metab. 19 (3), 380–392. https://doi.org/10.1016/j.cmet.2014.01.002.

Mano, S., Nishimura, M., 2005. Plant Peroxisomes. Plant Hormones. Elsevier, pp. 111–154.

Massudi, H., Grant, R., Guillemin, G.J., Braidy, N., 2012. NAD^+ metabolism and oxidative stress: the golden nucleotide on a crown of thorns. Redox Rep. 17 (1), 28–46. https://doi.org/10.1179/1351000212y.0000000001.

Mhamdi, A., Queval, G., Chaouch, S., Vanderauwera, S., Van Breusegem, F., Noctor, G., 2010. Catalase function in plants: a focus on Arabidopsis mutants as stress-mimic models. J. Exp. Bot. 61 (15), 4197–4220. https://doi.org/10.1093/jxb/erq282.

Mhamdi, A., Noctor, G., Baker, A., 2012. Plant catalases: peroxisomal redox guardians. Arch. Biochem. Biophys. 525 (2), 181–194. https://doi.org/10.1016/j.abb.2012.04.015.

Mittler, R., Vanderauwera, S., Gollery, M., Van Breusegem, F., 2004. Reactive oxygen gene network of plants. Trends Plant Sci. 9 (10), 490–498. https://doi.org/10.1016/j.tplants.2004.08.009.

Noctor, G., Foyer, C.H., 1998. Ascorbate and glutathione: keeping active oxygen under control. Annu. Rev. Plant Physiol. 49, 249–279. https://doi.org/10.1146/annurev.arplant.49.1.249.

Noctor, G., Veljovic-Jovanovic, S., Driscoll, S., Novitskaya, L., Foyer, C.H., 2002. Drought and oxidative load in the leaves of C3 plants: a predominant role for photorespiration? Ann. Bot. 89, 841–850. https://doi.org/10.1093/aob/mcf096. Spec No(7).

Noctor, G., Mhamdi, A., Chaouch, S., Han, Y., Neukermans, J., Marquez-Garcia, B., Queval, G., Foyer, C.H., 2012. Glutathione in plants: an integrated overview. Plant Cell Environ. 35 (2), 454–484. https://doi.org/10.1111/j.1365-3040.2011.02400.x.

Noctor, G., Lelarge-Trouverie, C., Mhamdi, A., 2015. The metabolomics of oxidative stress. Phytochemistry 112, 33–53. https://doi.org/10.1016/j.phytochem.2014.09.002.

Okumoto, K., El Shermely, M., Natsui, M., Kosako, H., Natsuyama, R., Marutani, T., Fujiki, Y, 2020. The peroxisome counteracts oxidative stresses by suppressing catalase import via Pex14 phosphorylation. eLife 9. https://doi.org/10.7554/elife.55896.

Omoto, E., Iwasaki, Y., Miyake, H., Taniguchi, M., 2016. Salinity induces membrane structure and lipid changes in maize mesophyll and bundle sheath chloroplasts. Physiol. Plant. 157 (1), 13–23. https://doi.org/10.1111/ppl.12404.

Palma, J.M., Mateos, R.M., López-Jaramillo, J., Rodríguez-Ruiz, M., González-Gordo, S., Lechuga-Sancho, A.M., Corpas, F.J, 2020. Plant catalases as NO and H_2S targets. Redox. Biol. 34, 101525 https://doi.org/10.1016/j.redox.2020.101525.

Pan, R., Liu, J., Wang, S., Hu, J, 2020. Peroxisomes: versatile organelles with diverse roles in plants. New Phytol. 225 (4), 1410–1427. https://doi.org/10.1111/nph.16134.

Pan, Y., Cheng, J.H., Sun, D.W., 2021. Metabolomic analyses on microbial primary and secondary oxidative stress responses. Compr. Rev. Food Sci. Food Saf. 20 (6), 5675–5697. https://doi.org/10.1111/1541-4337.12835.

Parnaud, G., Pignatelli, B., Peiffer, G., Taché, S., Corpet, D.E., 2000. Endogenous N-nitroso compounds, and their precursors, present in bacon, do not initiate or promote aberrant crypt foci in the colon of rats. Nutr. Cancer 38 (1), 74–80. https://doi.org/10.1207/S15327914NC381_11.

Rojas, C.M., Senthil-Kumar, M., Wang, K., Ryu, C.M., Kaundal, A., Mysore, K.S., 2012. Glycolate oxidase modulates reactive oxygen species–sediated signal transduction during nonhost resistance in *Nicotiana benthamiana* and Arabidopsis. Plant Cell 24 (1), 336–352. https://doi.org/10.1105/tpc.111.093245.

Salvi, P., Manna, M., Kaur, H., Thakur, T., Gandass, N., Bhatt, D., Muthamilarasan, M., 2021. Phytohormone signaling and crosstalk in regulating drought stress response in plants. Plant Cell Rep. 40 (8), 1305–1329. https://doi.org/10.1007/s00299-021-02683-8.

Schmid-Siegert, E., Stepushenko, O., Glauser, G., Farmer, E.E., 2016. Membranes as atructural ntioxidants: recycling of malondialdehyde to its source in oxidation-sensitive chloroplast fatty acids. J. Biol. Chem. 291 (25), 13005–13013. https://doi.org/10.1074/jbc.M116.729921.

Sies, H., 2015. Oxidative stress: a concept in redox biology and medicine. Redox Biol. 4, 180–183. https://doi.org/10.1016/j.redox.2015.01.002.

Sinha, T., Naash, M.I., Al-Ubaidi, M.R., 2020. Flavins act as a critical liaison between metabolic homeostasis and oxidative stress in the retina. Front. Cell Dev. Biol. 8 https://doi.org/10.3389/fcell.2020.00861.

Smirnoff, N., Arnaud, D., 2019. Hydrogen peroxide metabolism and functions in plants. New Phytol. 221 (3), 1197–1214. https://doi.org/10.1111/nph.15488.

Villate, A., San Nicolas, M., Gallastegi, M., Aulas, P.A., Olivares, M., Usobiaga, A., Etxebarria, N., Aizpurua-Olaizola, O., 2021. Review: metabolomics as a prediction tool for plants performance under environmental stress. Plant Sci. 303, 110789 https://doi.org/10.1016/j.plantsci.2020.110789.

Walter, T., Erdmann, R., 2019. Current advances in protein import into peroxisomes. Protein J. 38 (3), 351–362. https://doi.org/10.1007/s10930-019-09835-6.

Wanders, R.J.A., Ferdinandusse, S., Brites, P., Kemp, S., 2010. Peroxisomes, lipid metabolism and lipotoxicity. Biochim. Biophys. Acta Mol. Cell Biol. Lipids 1801 (3), 272–280. https://doi.org/10.1016/j.bbalip.2010.01.001.

Wang, S., Uddin, M.I., Tanaka, K., Yin, L., Shi, Z., Qi, Y., Mano, J., Matsui, K., Shimomura, N., Sakaki, T., Deng, X., Zhang, S., 2014. Maintenance of chloroplast structure and function by overexpression of the rice monogalactosyldiacylglycerol synthase gene leads to enhanced salt tolerance in tobacco. Plant Physiol. 165 (3), 1144–1155. https://doi.org/10.1104/pp.114.238899.

Xia, J., Psychogios, N., Young, N., Wishart, D.S, 2009. MetaboAnalyst: a web server for metabolomic data analysis and interpretation. Nucleic Acids Res. 37, 652–660. https://doi.org/10.1093/nar/gkp356.

Yamamoto, H., Fujimori, T., Sato, H., Ishikawa, G., Kami, K., Ohashi, Y, 2014. Statistical hypothesis testing of factor loading in principal component analysis and its application to metabolite set enrichment analysis. BMC Bioinform. 15, 51. https://doi.org/10.1186/1471-2105-15-51.

Yoshida, Y., Niki, E, 2004. Detection of lipid peroxidation *in vivo*: total hydroxyoctadecadienoic acid and 7-hydroxycholesterol as oxidative stress marker. Free Radic. Res. 38 (8), 787–794. https://doi.org/10.1080/10715760410001700460.

Yoshida, Y., Umeno, A., Shichiri, M., 2013. Lipid peroxidation biomarkers for evaluating oxidative stress and assessing antioxidant capacity *in vivo*. J. Clin. Biochem. Nutr. 52 (1), 9–16. https://doi.org/10.3164/jcbn.12-112.

FISCAL YEAR 2023 – 2024

FINANCIAL REPORT

January 1, 2023 – March 31, 2024

QUARTERLY REPORT

TOBACCO RESEARCH INCOME
INCOME COMPARISON

Fiscal Years	2017-2018	2018-2019	2019-2020	2020-2021	2021-2022	2022-2023	2023-2024
July	$ 2,459.48	$ 120,890.40	$ 141,864.01	$ 136,565.92	$ 102,816.87	$ 113,853.04	$ -
August	$ 292,266.42	$ 126,982.37	$ 145,789.42	$ 11,873.82	$ 148,863.59	$ 121,485.75	$ 225,154.79
September	$ 139,414.92	$ 178,553.92	$ 132,169.60	$ 261,157.23	$ 138,395.19	$ 143,503.64	$ 114,761.92
1st QUARTER	**$ 434,140.82**	**$ 426,426.69**	**$ 419,823.03**	**$ 409,596.97**	**$ 390,075.65**	**$ 378,842.43**	**$ 339,916.71**
October	$ 126,862.91	$ 97,793.84	$ 150,849.00	$ 141,682.93	$ 138,913.78	$ 131,512.77	$ 97,021.98
November	$ 123,267.74	$ 128,963.50	$ 117,280.34	$ 135,157.14	$ 101,844.54	$ 101,050.68	$ 132,736.05
December	$ 135,314.04	$ 175,277.00	$ 151,323.23	$ 159,616.92	$ 138,232.14	$ 113,515.64	$ 81,648.61
2nd QUARTER	**$ 385,444.69**	**$ 402,034.34**	**$ 419,452.57**	**$ 436,456.99**	**$ 378,990.46**	**$ 346,079.09**	**$ 311,406.64**
January	$ 127,719.90	$ 564,217.88	$ 120,247.87	$ 93,056.96	$ 116,044.01	$ 111,657.62	$ 101,501.91
February	$ 114,047.53	$ 141,118.46	$ 114,095.14	$ 125,797.09	$ 89,271.71	$ 78,955.86	$ 74,500.35
March	$ 159,645.83	$ 122,472.86	$ 403,962.17	$ 143,903.75	$ 140,521.53	$ 119,175.49	$ 105,636.69
3rd QUARTER	**$ 401,413.26**	**$ 827,809.20**	**$ 638,305.18**	**$ 362,757.80**	**$ 345,837.25**	**$ 309,788.97**	**$ 281,638.95**
April	$ 65,036.15	$ 146,789.57	$ 117,862.64	$ 144,970.47	$ 127,449.97	$ 79,639.90	$ -
May	$ 209,087.27	$ 63,797.02	$ 141,525.18	$ 100,238.76	$ 148,769.94	$ 120,890.24	$ -
June	$ 168,621.20	$ 250,352.13	$ 138,849.18	$ 211,130.06	$ 121,204.33	$ 133,854.96	$ -
4th QUARTER	**$ 442,744.62**	**$ 460,938.72**	**$ 398,237.00**	**$ 456,339.29**	**$ 397,424.24**	**$ 334,385.10**	**$ -**
TOTAL INCOME	**$ 1,663,743.39**	**$ 2,117,208.95**	**$ 1,875,817.78**	**$ 1,665,151.05**	**$ 1,512,327.60**	**$ 1,369,095.59**	**$ 932,962.30**

FISCAL YEAR 2023-2024 **INCOME AND FINANCIAL REPORT** **KTRDC 3rd QUARTER REPORT**

Funds Center	Funds Center Name	Commitment	Annual Budget	Prior Month Balance	Current Month Actual	YTD Actual	YTD Encumbrances	Available Budget
1235410080	KTRDC HOLDING AC	Revenue	($2,200,000.00)	($827,325.61)	($94,181.16)	($921,506.77)		($1,278,493.23)
1235410080	Result	Total	($2,200,000.00)	($827,325.61)	($94,181.16)	($921,506.77)		($1,278,493.23)
1235410090	KENTUCKY TOBACC	Operating Expenses	$1,000.00		$199.03	$199.03		$800.97
1235410090	KENTUCKY TOBACC	Recharges			$1.43	$1.43		($1.43)
1235410090	Result	Total	$1,000.00		$200.46	$200.46		$799.54
1235410100	KTRDC ADMINISTRAT	Salaries	$288,500.00	$111,395.03	$13,532.59	$124,927.62	$43,400.41	$120,171.97
1235410100	KTRDC ADMINISTRAT	Benefits		$26,701.95	$3,444.75	$30,146.70	$12,940.14	($43,086.84)
1235410100	KTRDC ADMINISTRAT	Operating Expenses		$6,871.87	$4,395.00	$11,266.87	$135.78	($11,402.65)
1235410100	KTRDC ADMINISTRAT	Recharges		$14,199.73	$2,154.87	$16,354.60		($16,354.60)
1235410100	Result	Total	$288,500.00	$159,168.58	$23,527.21	$182,695.79	$56,476.33	$49,327.88
1235410110	KTRDC PERSONNEL	Salaries	$1,169,300.00	$598,262.72	$78,059.70	$676,322.42	$202,391.82	$290,585.76
1235410110	KTRDC PERSONNEL	Benefits		$170,379.85	$21,584.66	$191,964.51	$65,464.47	($257,428.98)
1235410110	KTRDC PERSONNEL	Operating Expenses		$248.00	$31.00	$279.00		($279.00)
1235410110	KTRDC PERSONNEL	Expense Transfers		$2,565.05	$449.53	$3,014.58		($3,014.58)
1235410110	KTRDC PERSONNEL	Recharges		$30,487.25	$3,746.08	$34,233.33		($34,233.33)
1235410110	Result	Total	$1,169,300.00	$801,942.87	$103,870.97	$905,813.84	$267,856.29	($4,370.13)
1235410120	KTRDC PUBLICATION	Operating Expenses	$40,000.00	$2,790.00	$7,598.83	$10,388.83		$29,611.17
1235410120	KTRDC PUBLICATION	Recharges		$799.79	$112.46	$912.25		($912.25)
1235410120	Result	Total	$40,000.00	$3,589.79	$7,711.29	$11,301.08		$28,698.92
1235410130	KTRDC BUILDING MA	Operating Expenses	$70,000.00	$20,085.80	$2,222.26	$22,308.06	$1,211.53	$46,480.41
1235410130	KTRDC BUILDING MA	Recharges		$9,656.24	$305.95	$9,962.19		($9,962.19)
1235410130	Result	Total	$70,000.00	$29,742.04	$2,528.21	$32,270.25	$1,211.53	$36,518.22
1235410180	KTRDC SHOP	Operating Expenses	$2,000.00	$577.92	$45.46	$623.38	$27.40	$1,349.22
1235410180	KTRDC SHOP	Recharges		$1.79	$0.53	$2.32		($2.32)
1235410180	Result	Total	$2,000.00	$579.71	$45.99	$625.70	$27.40	$1,346.90

FISCAL YEAR 2023-2024 **INCOME AND FINANCIAL REPORT** **KTRDC 3rd QUARTER REPORT**

Funds Center	Funds Center Name	Commitment	Annual Budget	Prior Month Balance	Current Month Actual	YTD Actual	YTD Encumbrances	Available Budget
1235410240	KTRDC LABORATORY	Operating Expenses	$44,200.00	$74,856.31	$1,693.06	$76,549.37	$0.00	($32,349.37)
1235410240	KTRDC LABORATORY	Recharges		$714.31		$714.31		($714.31)
1235410240	Result	Total	$44,200.00	$75,570.62	$1,693.06	$77,263.68	$0.00	($33,063.68)
1235410250	KTRDC UNALLOCATE	Operating Expenses	$90,000.00					$90,000.00
1235410250	Result	Total	$90,000.00					$90,000.00
1235410280	KTRDC GENERAL LAB	Operating Expenses	$125,000.00	$13,330.57	$11,034.43	$24,365.00	$4,749.83	$95,885.17
1235410280	KTRDC GENERAL LAB	Recharges		$240.64	$571.96	$812.60		($812.60)
1235410280	Result	Total	$125,000.00	$13,571.21	$11,606.39	$25,177.60	$4,749.83	$95,072.57
1235411040	KTRDC DISCRETIONA	Operating Expenses	$10,000.00	$8,609.29	$1,074.13	$9,683.42		$316.58
1235411040	KTRDC DISCRETIONA	Recharges		$89.60	$8.95	$98.55		($98.55)
1235411040	Result	Total	$10,000.00	$8,698.89	$1,083.08	$9,781.97		$218.03
1235411310	KTRDC OUTREACH &	Operating Expenses	$30,000.00					$30,000.00
1235411310	Result	Total	$30,000.00					$30,000.00
1235411320	KTRDC PLANT GENET	Salaries		$19,523.83		$19,523.83		($19,523.83)
1235411320	KTRDC PLANT GENET	Benefits		$8,025.68		$8,025.68		($8,025.68)
1235411320	KTRDC PLANT GENET	Operating Expenses	$30,000.00					$30,000.00
1235411320	KTRDC PLANT GENET	Recharges		$66.18		$66.18		($66.18)
1235411320	Result	Total	$30,000.00	$27,615.69		$27,615.69		$2,384.31
1235411340	GENETIC MANIPULAT	Salaries		$16,516.60		$16,516.60		($16,516.60)
1235411340	GENETIC MANIPULAT	Benefits		$5,141.22		$5,141.22		($5,141.22)
1235411340	GENETIC MANIPULAT	Operating Expenses	$30,000.00	$4,107.50		$4,107.50	$0.00	$25,892.50
1235411340	GENETIC MANIPULAT	Recharges		$986.34		$986.34		($986.34)
1235411340	Result	Total	$30,000.00	$26,751.66		$26,751.66	$0.00	$3,248.34
1235411360	PLANT BIOTECH MET	Operating Expenses	$30,000.00	$6,051.64	$2,572.40	$8,624.04	$14,308.10	$7,067.86
1235411360	PLANT BIOTECH MET	Recharges		$38.50	$24.44	$62.94		($62.94)
1235411360	Result	Total	$30,000.00	$6,090.14	$2,596.84	$8,686.98	$14,308.10	$7,004.92

FISCAL YEAR 2023-2024 **INCOME AND FINANCIAL REPORT** **KTRDC 3rd QUARTER REPORT**

Funds Center	Funds Center Name	Commitment	Annual Budget	Prior Month Balance	Current Month Actual	YTD Actual	YTD Encumbrances	Available Budget
1235411370	KTRDC PLANT BIOTE	Operating Expenses	$30,000.00	$22,194.19	$1,578.27	$23,772.46	$148.14	$6,079.40
1235411370	KTRDC PLANT BIOTE	Recharges		$3,772.97	$34.94	$3,807.91		($3,807.91)
1235411370	Result	Total	$30,000.00	$25,967.16	$1,613.21	$27,580.37	$148.14	$2,271.49
1235411380	MOLECULAR GENETI	Operating Expenses	$30,000.00	$17,415.24	$874.65	$18,289.89	$0.00	$11,710.11
1235411380	MOLECULAR GENETI	Recharges		$2,330.74	$13.62	$2,344.36		($2,344.36)
1235411380	Result	Total	$30,000.00	$19,745.98	$888.27	$20,634.25	$0.00	$9,365.75
1235411410	KTRDC GREENHOUSI	Operating Expenses	$30,000.00	$1,688.08	$20.85	$1,708.93	$65.83	$28,225.24
1235411410	KTRDC GREENHOUSI	Recharges		$2,191.37	$256.35	$2,447.72	$0.00	($2,447.72)
1235411410	Result	Total	$30,000.00	$3,879.45	$277.20	$4,156.65	$65.83	$25,777.52
1235411430	PLANT ANALYTIC RES	Operating Expenses	$30,000.00		$903.19	$903.19	$1,550.00	$27,546.81
1235411430	PLANT ANALYTIC RES	Recharges			$10.52	$10.52		($10.52)
1235411430	Result	Total	$30,000.00		$913.71	$913.71	$1,550.00	$27,536.29
1235411570	TOBACCO MOLECUL	Operating Expenses	$30,000.00	$1,107.91	$1,444.27	$2,552.18	$0.00	$27,447.82
1235411570	TOBACCO MOLECUL	Recharges		$3,083.12	$4,104.47	$7,187.59		($7,187.59)
1235411570	Result	Total	$30,000.00	$4,191.03	$5,548.74	$9,739.77	$0.00	$20,260.23
1235411640	GENE DISCOVERY	Salaries		$13,259.20	$1,657.40	$14,916.60	$4,972.20	($19,888.80)
1235411640	GENE DISCOVERY	Benefits		$4,775.51	$596.94	$5,372.45	$1,815.48	($7,187.93)
1235411640	GENE DISCOVERY	Operating Expenses	$30,000.00					$30,000.00
1235411640	Result	Total	$30,000.00	$18,034.71	$2,254.34	$20,289.05	$6,787.68	$2,923.27
1235412240	GREENHOUSE EVALU	Salaries		$27,522.30		$27,522.30		($27,522.30)
1235412240	GREENHOUSE EVALU	Benefits		$6,569.89		$6,569.89		($6,569.89)
1235412240	GREENHOUSE EVALU	Operating Expenses	$30,000.00					$30,000.00
1235412240	Result	Total	$30,000.00	$34,092.19		$34,092.19		($4,092.19)

FISCAL YEAR 2023-2024 **INCOME AND FINANCIAL REPORT** **KTRDC 3rd QUARTER REPORT**

Funds Center	Funds Center Name	Commitment	Annual Budget	Prior Month Balance	Current Month Actual	YTD Actual	YTD Encumbrances	Available Budget
1235412360	FLAVONOID - SMALL	Salaries		$11,989.23		$11,989.23		($11,989.23)
1235412360	FLAVONOID - SMALL	Benefits		$3,599.13		$3,599.13		($3,599.13)
1235412360	FLAVONOID - SMALL	Operating Expenses	$30,000.00	$458.01	$1.77	$459.78		$29,540.22
1235412360	FLAVONOID - SMALL	Recharges		$0.66	$0.71	$1.37		($1.37)
1235412360	Result	Total	$30,000.00	$16,047.03	$2.48	$16,049.51		$13,950.49

Kentucky Tobacco
Research & Development Center